Ph. D. Thesis

The utility of active growth factors encapsulated in microcrystals produced in insect cell lines and individual silkworms

Rina Maruta

2021

Kyoto Institute of Technology

Abstract

In clinical settings, medications containing growth factors currently suffer problems with safety and cost because they require high doses and repeated administration over long or short periods due to the short half-life of the growth factors. To address these issues, polyhedra microcrystals derived from the insect-infecting cypovirus 1 within the Reoviridae family were developed. Such polyhedra can be used as vehicles to protect and release encapsulated cell growth factors. As described in Chapter 2, I successfully produced nerve growth factor (NGF)-encapsulating polyhedra (pNGF). These were spotted onto a coverslip to create a uniform circular field; the alignment of differentiated rat neuronal precursor cells (PC12 cells) via their extended axons along the periphery of the pNGF circular field was observed. In addition, I attempted to elucidate the mechanism of cytokine release from polyhedra by investigating whether matrix metalloproteinases (MMPs) secreted from mammalian cells degrade polyhedra. I found that the release of NGF from pNGF was promoted by MMPs secreted from PC12 cells. To date, polyhedra have been produced in baculovirus-infected *Spodoptera frugiperda* IPLB-SF21-AE cells (Sf21 cells); however, for the purposes of safe medical use in humans, polyhedra should be produced in a virus-free and serum-free system. To produce recombinant polyhedra in such a system, I attempted to generate transgenic silkworms that express target protein-

encapsulating polyhedra in their silk glands, which are known to produce fibroin biopolymer (a highly biodegradable and biocompatible material). As detailed in Chapter 3, I generated transgenic silkworm that expresses FGF-7-encapsulating polyhedra (pFGF-7) in their middle and posterior silk glands. Continuous FGF-7 release from the processed posterior silk gland expressing pFGF-7 induced keratinocyte proliferation and enabled the construction of a human epidermal model. The results demonstrate that cytokine-encapsulating polyhedra produced from insect cell lines and individual silkworms could have valuable applications in cell/tissue engineering *in vivo* and *in vitro*.

Contents

Chapter 1

General Introduction

Growth factors are soluble, secreted proteins that regulate cellular responses during tissue regeneration. They are upregulated in response to tissue damage and are secreted by platelets, leukocytes, fibroblasts, and epithelial cells. Once secreted, growth factors bind to cellular receptors, activating a signal cascade to facilitate wound healing. Even at low concentrations, growth factors can induce cell migration, proliferation, and differentiation to regenerate tissue [1, 2]. There is reduced growth factor secretion in acute and chronic non-healing wounds, resulting in delayed wound healing. Thus, growth factors for treating such wounds are required to promote healing. Indeed, drug delivery of recombinant growth factors is supportive treatment in many surgical fields. However, the clinical application of recombinant growth factors is limited because of their short half-life *in vivo*, which is due to their low stability and elimination by exudation before reaching the wounds after topical application [1]. Several approved medications that include recombinant growth factors are available as preparations for external use in the form of solutions, creams, and gels. However, these medications require high doses and/or repeated administration over long or short periods that can cause severe side effects, including oncogenesis [2]. Furthermore, such high-dose growth factor medications can increase the cost of therapy. Overall, the safety and cost of growth factor-loaded drug delivery systems (DDSs) in clinical settings remain problematic [1, 2].

To address these problems, I developed cypovirus polyhedra microcrystals as biomaterials for DDSs. Cypoviruses, within the family Reoviridae, infect insects; the cells of infected insects then produce large amounts of virus-encoded proteins such as polyhedrin. Progeny virus particles occlude into crystallized polyhedrin, namely polyhedra, for protection against the severe environment [3]. Previously, I successfully developed a method of producing recombinant polyhedra that incorporates foreign proteins rather than virus particles [Publication List 1, 4–11]. This method uses partial sequences of polyhedrins or virus proteins as tags, e.g. H1-tags or VP3-tags, to encapsulate a variety of foreign proteins, such as fluorescence proteins [4-7], cytokines [Publication List 1, 8-10], and fusion proteins comprising enzymes [11], into polyhedra. This process fuses the H1-tag is to the N-terminus of the target foreign protein and fuses the VP3-tag to the C-terminus. Notably, the polyhedra retain the biological activity of the encapsulated foreign proteins for an extended period and release the proteins slowly [Publication List 2, 4]. For example, polyhedra can release biologically active cytokines continuously into the culture medium during co-incubation with mammalian cells; using a conditioned medium for the cell culture will induce this release [9, 10]. A previous study applied bone morphogenetic protein-2 (BMP-2)-encapsulating polyhedra (pBMP-2) to regenerate bone in rats [12]. This study implanted pBMP-2 with an absorbable collagen

sponge (ACS) in critical-sized bone defects and applied an ACS containing recombinant human BMP-2 (rhBMP-2) as a control. Although the ACS with rhBMP-2 induced some bone regeneration, the defect had not healed completely 15 weeks after implantation. In contrast, the ACS with pBMP-2 induced near-complete bone healing at 15 weeks, thoroughly digested the pBMP-2, and replaced it with newly generated bone. Importantly, there were neither inflammatory reactions nor other biological reactions in the host tissues adjacent to the polyhedra implantation site. This study's results demonstrate that polyhedra can release active BMP-2 over the long-term and that polyhedra-encapsulating growth factors are biocompatible and biodegradable materials for use as DDSs.

To produce foreign target protein-encapsulating polyhedra *in vitro*, two baculovirus vectors, containing *polyhedrin* and/or tag-fused target protein sequences, are placed into *Spodoptera frugiperda* (Sf21) cells [Publication List 1, 4–11]. Using this method, I successfully produced polyhedra that encapsulated active nerve growth factor (NGF) [Publication List 1], an essential neurotrophic factor for the growth, maintenance and survival of target neurons, as well as for regeneration of peripheral nerve cells. NGF is known to support the rat neuronal precursor cell (PC12 cell) differentiation and induce axonal growth in a dose-dependent manner [13]. I spotted NGF-encapsulating polyhedra (pNGF) onto a coverslip and observed the alignment of PC12 cells with the extension of

their axons along the periphery of the spot. In contrast, soluble NGF induced only a random extension of PC12 cell axons [Publication List 1]; random extension of axons is disadvantageous for nerve regeneration and should be minimized if possible [13]. Indeed, a previous study showed that significant induction of neurite outgrowth was observed in aligned differentiated nerve cells when compared with randomly oriented nerve cells [14].

For cell growth factor-encapsulating polyhedra to be clinically applicable, the polyhedra must be produced in a virus-free and serum-free system. Baculoviruses can internalize within mammalian cells via stimulation of cell endocytosis or pinocytosis and by the action of envelope glycoproteins. Thus, such viruses can functionally influence the mammalian innate immune response [15]. Additionally, cell culture systems can, on occasion, include pathogenic serum. Therefore, to safely produce recombinant polyhedra under virus-free and serum-free conditions, I attempted to generate transgenic silkworms that express target proteins encapsulated in polyhedra in their middle silk glands (MSGs) and posterior silk glands (PSGs) [Publication List 2–3]. In the present study, I specifically used fibroblast growth factor-7 (FGF-7) and polyhedra to induce keratinocyte proliferation. This proliferation and migration is pivotal for re-epithelialization of the skin during wound healing [4]. The silk gland is an organ that synthesizes many silk proteins, such as sericin and fibroin, during the construction of the silkworm cocoon. The cocoon's

main component, fibroin biopolymer, is expressed in the PSG. It is a highly biodegradable and biocompatible material [16-24]. In general, silk glands have a high capacity for protein synthesis, which can be applied in protein engineering [16, 17]. I expected transgenic silkworms to express FGF-7-encapsulating polyhedra (pFGF-7) and thereby produce new silk materials that release FGF-7 over a long period.

FGF-7 has been used to establish a three-dimensional (3D) epidermal model [25] that can be used as a model of the human epidermis to substitute for *in vivo* animal tests. This model has been used successfully to assess skin irritation caused by acute toxicity [26, 27], allergenicity [28], and inflammatory effects of test compounds [29]. During construction of this epidermal model, keratinocytes are cultured on top of collagen gel and then submerged in a medium for two days. The keratinocytes are then exposed to air for 14 days to induce their differentiation into the epidermis. During their cultivation, keratinocytes need continuous supplementation of FGF-7; thus, the culture medium must be changed every 2–3 days. Frequent medium exchange increases the risk of contamination or cell damage and can inhibit the epidermis' proper formation. I expected that using the silk material processed from the pFGF-7–expressing silk gland would reduce the frequency at which the medium was changed and thereby facilitate the epidermal model's construction.

Previous study reported that co-incubating polyhedra with mammalian cells or their conditioned medium gradually released biologically active cytokines from the polyhedra [9, 10]. However, the cytokine release mechanism has yet to be elucidated. I hypothesized that proteases, probably matrix metalloproteinases (MMPs), secreted from mammalian cells degrade the polyhedra. MMPs are proteolytic enzymes from the zinc protease superfamily [30]. The MMP family is involved in the breakdown of the extracellular matrix in normal physiological processes such as embryonic development, reproduction, and tissue re-modeling [30, 31].

In Chapter 2, I describe the pNGF production and reveal that MMP-2 and MMP-8 mediated NGF release. Furthermore, I confirm that MMPs secreted by PC12 cells induce the release of NGF. When these pNGF were spotted onto a coverslip to create a uniform circular field, there was movement and alignment of PC12 cells via their extended axons along the periphery of the pNGF field. Neural cell differentiation was confirmed by the expression of specific markers of tau, neurofilament, and GAP-43. There were also connections between the extended axons and growth cones, and connexin 43 expression was consistent with gap junction formation. Extension and connection of very fine filopodia also occurred between growth cones. In Chapter 3, I describe the generation of transgenic silkworms that express pFGF-7 in their MSGs and PSGs.

Immunostaining showed that the polyhedra from silk glands are associated with FGF-7. Furthermore, the powder prepared from MSGs and PSGs retained FGF-7 activity and stimulated the proliferation of human keratinocyte epidermal cells. The FGF-7 activity of PSG powder was higher than that of MSG powder. Moreover, PSG powder released FGF-7 gradually over a long period, and it induced keratinocyte proliferation and differentiation to form a stratified epidermis in a 3D culture. Based on this evidence, I discuss the application of cytokine-encapsulating polyhedra produced in insect cell lines and individual silkworms via tissue engineering.

Chapter 2

Sustained Neurotrophin Release from Protein Nanoparticles Mediated by Matrix Metalloproteinases Induces the Alignment and Differentiation of Nerve Cells

Introduction

The development and maintenance of the human body requires many complex interactions between cells and components of the extracellular matrix (ECM), which creates the localized microenvironments responsible for tissue development homeostasis. Control of this cellular microenvironment is therefore important for developing tissue-engineered organ substitutes. To this end, significant efforts have been directed to investigate the capacity of biomaterials and scaffolds to support and control cell growth. A number of studies have addressed topographic guidance for regulation of cell shape, orientation and movement at the interface between cells and various components of the ECM [32–36]. It was originally thought that MMPs primarily functioned to degrade all components of the ECM and basement membrane for tissue remodeling and maintenance. However, it has also been demonstrated that MMPs regulate the release or activation of chemokines, cytokines, growth factors, and other bioactive molecules [37]. Concentration gradients of growth factors released by MMPs are also important in tissue development, and significant efforts, for example using microfluidics [38], have been focused on the development of devices that can maintain stable concentration gradients of recombinant growth factors *in vitro*.

Traumatic central and peripheral nerve injury may lead to a substantial loss of

nerve tissue between the proximal and the distal nerve stump. Consequently, extensive efforts have been made over the past few decades to develop treatment methods for nerve regeneration. The use of ECM mimetics, which utilize collagen gel compaction, electromagnetic fields, electrospinning of nanofibers, mechanical stimulation and microstructured culture plates for artificial guidance of nerve cells, have all been explored [39–42]. However, such artificial ECM mimetics have not led to effective therapies to address nerve injury and disease.

Previous studies have demonstrated that NGF, a member of the neurotrophin family, promotes the survival and differentiation of sensory and sympathetic neurons and may have the potential to be utilized for artificial guidance of nerve cells [43,44]. When PC12 cells, a rat neuronal precursor cell line, which has been widely used as a model for neural differentiation, are cultured in the presence of recombinant NGF, neuronal differentiation to cells that resemble sympathetic neurons, both morphologically and functionally, is observed [45]. However, the neurite outgrowth that is typically observed sprouting from the cell body lacks directionality due to the homogeneous dispersion of NGF throughout the culture medium. It would be desirable to deliver NGF to the vicinity of neuronal cells by a simple, self-sustaining sustained-release mechanism that would create, over time, a similar stable microenvironment achieved by physiological supply

from the ECM.

Micron-sized proteinaceous particles, known as polyhedra, are the main vectors by which virus particles transfer from insect to insect [46]. By incorporating virus particles into their crystalline superstructure, polyhedra stabilize these virions, thereby allowing them to remain viable in the external environment for long periods of time. developed two targeted strategies for the encapsulation of foreign proteins into Bombyx mori cypovirus 1 (CPV) polyhedra [4]. Specifically, diverse foreign proteins can be encapsulated into polyhedra by fusing a polyhedra-targeting tag sequence to the C- or N-terminus of the cargo proteins. The remarkable stability of polyhedra suggests that these systems could be robust as sustained-release carriers of cytokines and other proteins for tissue engineering or vaccination applications [4]. Moreover, polyhedrin nanoparticles are inert and insoluble in physiological conditions, allowing for polyhedra to be employed as versatile micron-sized carriers.

Here, I report the development and use of pNGF which generate slow and sustained release of NGF to direct the behavior of PC12 cells.

Materials and Methods

Assays for MMPs

I evaluated MMP-1, -9, and -12 (Sino Biological Inc.) and MMP-2, -3, -7, and -8 (Life Laboratory). MMP-2, -3, -7, and -8 were in their active form, whereas MMP-1, -9, and -12 required activating by chymotrypsin. MMP-1 (5 ng/μL), MMP-2, -3, and -7 (0.00025 units/μL), MMP-8 (0.00035 units/μL), MMP-9 (5 ng/μL), and MMP-12 (10 ng/μL) were added to 5×10^6 pEGFP in 100 μL of TCNB buffer (5 mM Tris pH 7.5, 1 mM $CaCl_2$, 15 mM NaCl, 0.005% Brij-35). After incubation for 72 h at 35°C, reactions were stopped by adding 12 μL of 0.5 M EDTA (pH 8.0). Subsequently, supernatants were collected by centrifugation and the fluorescence was measured (Ex/Em = 485/538) (Fluoroskan Ascent, Thermo Fisher Scientific, Waltham, WA, USA). The assays were carried out in triplicate.

Conditioned medium from culturing PC12 cells in various conditions was recovered and the proteins were concentrated by acetone precipitation. Subsequently, the samples were resolved by 12.5% SDS-PAGE and transferred to a nitrocellulose membrane at 2 mA/cm^2 for 20 min. The membranes were treated with primary antibody (anti-MMP-2 antibody (Proteintech) with a 1:1000 dilution and anti-MMP-8 antibody (Boster Biological Technology) with a 1:2000 dilution) and incubated for 16 h at 4°C.

After washing three times, the membrane was incubated with a 1:2500 dilution of goat anti-rabbit IgG conjugated to horseradish peroxidase (Bio-Rad) for 2 h at room temperature. Results were visualized by Chemilumi-One (Nacalai Tesque, Kyoto, Japan).

RT-PCR

The expression of MMP-1, -2, -3, -7 and -8 mRNAs was analyzed by RT-PCR and qPCR. PC12 cells were cultured in DMEM containing pNGF (8×10^5 cubes /mL) or NGF-2.5S (100 ng/mL) for 5 days. PC12 cells were also cultured in DMEM only as a control. The cDNA from cells in each culture were prepared by reverse transcription (Revert Aid reverse transcriptase, Thermo Fisher Scientific, Waltham, WA, USA) from total RNA isolated using spin columns (Favor Prep^{TM}, FAVORGEN, Ping-Tung, Taiwan). Products of RT-PCR were analyzed by gel electrophoresis. Specific primers used for qPCR are listed below. MMP-1 Forward; TTGCTTCTCTTGGCTACCAGCTCA, MMP-1 Reverse; TAGCTTGGACGTCTTCACCCAAGT, MMP-2 Forward; TGGGGGAGATTCTCACTTTG, MMP-2 Reverse; CCATCAGCGTTCCCATACTT, MMP-3 Forward; TGGGAAGCCAGTGGAAATG, MMP-3 Reverse; CCATGCAATGGGTAGGATGAG, MMP-7 Forward; TCGGCGGAGATGCTCACT, MMP-7 Reverse; TGGCAACAAACAGGAAGTTCAC, MMP-8 Forward;

ACCTACGAAAATTCTACCACTTACCAA, MMP-8 Reverse; CCTTAAGCTTCTCGGCAATCA, GAPDH Forward; ACAGTCCATGCCATCACTGCC, GAPDH Reverse; GCCTGCTTCACCACCTTCTTG, Actin Forward; ATTGCTGACAGGATGCAGAA, Actin Reverse; TAGAGCCACCAATCCACACAG.

Construction of Expression Vectors for pNGF

The cDNA encoding the NGF ORF was purchased from Toyobo in a GATEWAY® entry clone. The full-length (241 amino acids) and mature (120 amino acids) forms of NGF were subcloned into each destination vector (pDEST/VP3, and pDEST/H1) [16], resulting in production of the transfer vectors encoding the full-length or mature form of NGF fused with VP3 or H1 tags (pTransH1/full NGF, pTransH1/mature NGF, pTransVP3/full NGF, and pTransVP3/mature NGF). These transfer vectors were co-transfected into Sf21 insect cells with Baculo Gold^{TM} baculovirus linearized DNA. After incubation for 5 days at 27 °C, recombinant baculoviruses expressing the full-length and mature forms of NGF fused with VP3 or H1 tags were harvested and stored at 4 °C.

Expression and Purification of pNGF

To generate polyhedra consisting of only BmCPV polyhedrin (empty polyhedra), Spodoptera frugiperda IPLB-SF21-AE cells (Sf cells) were inoculated with recombinant baculovirus AcCP-H29 expressing BmCPV polyhedrin under the control of the baculovirus *polyhedrin* promoter. For production of pNGF, Sf cells were co-infected with AcCP-H29 and an additional recombinant baculovirus expressing recombinant NGF fused with either VP3 or H1 tags [4]. The infected cells were cultured for 10 days at 27 °C and then harvested in a conical tube by centrifugation. The cell pellet was resuspended in phosphate-buffered saline (PBS; pH 7.2) and treated with an ultrasonic homogenizer at 6% power for 30 s. The cell homogenate was centrifuged at 1500 × g at 4 °C and the supernatant was removed. These treatments were repeated, and the purification was complete. The polyhedra suspension was adjusted to 5×10^4 or 1×10^5 cubes /μL and stored at 4 °C in distilled water containing 100 units/mL penicillin and 100 μg/mL streptomycin.

Cover Slip Coating

Cover slips (φ 12 mm) (Fisher Scientific) were sterilized with 70% ethanol and subsequently washed with sterilized water. Cellmatrix Type IV (Nitta Gelatin) was dissolved in 0.15 M acetic acid (30 μg/mL). The sterilized cover slips were placed in the

culture wells and 0.5 mL of Cellmatrix Type IV solution was then added. Following overnight incubation, the Cellmatrix Type IV solution was discarded and the cover slips were allowed to dry for 1 h. Collagen-coated cover slips were washed twice with serum-free DMEM. One microliter of polyhedra suspension (5×10^4 or 1×10^5 cubes /μL) was spotted on the cover slips and allowed to dry for at least 3 h.

PC12 Cell Culture

PC12 cells (RCB0009 RIKEN BRC) were cultured with DMEM culture medium supplemented with 10% fetal bovine serum and 10% horse serum. The cell culture medium was discarded and 0.02% EDTA solution was added. After the EDTA solution was discarded, 1 mL of 0.25% trypsin-EDTA was added and incubated for 1 min. One milliliter of DMEM culture medium was added and the cell suspension was centrifuged at 1200 rpm for 2 min. After discarding the supernatant, cells were suspended in 1 mL of serum-free DMEM and the number of cells was counted. Cells (7×10^4 cells/well) were then seeded into a well and incubated with serum-free DMEM medium for 5 days without medium exchange. Images of cell alignment were obtained via scanning electron microscopy (SEM) on the 5th day following cell seeding. The NGF 2.5S subunit (NGF-2.5S) from murine submaxillary glands (Sigma Aldrich, Darmstadt, Germany) was also

used as a control.

Preparation of Cells for SEM Imaging

After gently discarding the cell medium, cells were fixed with 4% paraformaldehyde phosphate buffer solution, 1% osmium tetroxide and 1% tannic. Dehydration was carried out by immersing the cover slips in a series of ethanol solutions of increasing concentrations until 100% dehydration was achieved. Cover slips were covered with hexamethyldisilazane and allowed to dry overnight. Images of cell alignment were obtained via SEM after gold-sputtering (200 Å).

Immunocytochemistry

For immunofluorescence, cells on the cover slips were fixed for 30 min at room temp with 4% paraformaldehyde. After three washes with PBS for 5 min each, the cells were permeabilized with 0.3% Triton X-100 in PBS for 15 min at room temperature. After three washes with PBS for 5 min each, the cells were incubated in blocking buffer (3% FBS in PBS) for 1 h at room temperature and then incubated with primary antibodies (anti-tau antibody (Merck Millipore, Darmstadt, Germany), anti-neurofilament heavy polypeptide antibody (Sigma Aldrich, Darmstadt, Germany), anti-GAP-43 antibody (Merck Millipore,

Darmstadt, Germany), and anti-connexin 43 antibody (Invitrogen, Thermo Fisher Scientific, Waltham, WA, USA) overnight at 4 °C. After three washes with PBS for 10 min each, the cells were incubated with FITC-conjugated secondary antibody (goat anti-mouse IgG antibody (Invitrogen) for 1 h at room temperature. Cover slips were then washed three times with PBS and finally mounted on microscope slides in mounting medium with propidium iodide (Invitrogen) for nuclei staining. Stained cells were observed using an Olympus Fluoview FV1000-IX81 confocal microscope (Olympus, Tokyo, Japan).

Results

Release of Cargo Proteins from polyhedrin micro-crystals

Previous study have reported that biologically active cytokines are sustainably released from polyhedra, when the polyhedra are co-incubated with mammalian cells or conditioned medium [9, 10]. However, the mechanism by which release is mediated had not been elucidated.

I hypothesized that the degradation of the polyhedra is achieved by proteases, specifically MMPs, secreted by nearby PC12 cells. MMPs are proteolytic enzymes belonging to the zinc protease superfamily that has several sub-groups. These include collagenase (MMP-1, -8, -13), gelatinase (MMP-2, -9), stromelysin (MMP-3, -10, -11), matrilysin (MMP-7), and other membrane associated MMPs [30]. The MMP family is involved in the breakdown of ECM in normal physiological processes, such as embryonic development, reproduction, and tissue remodeling. MMPs are secreted as inactive pro-proteins but are activated when cleaved by extracellular proteinases [10, 16].

To investigate whether selected MMPs from across several sub-groups do indeed degrade polyhedra, enhanced green fluorescent protein (EGFP) was incorporated into polyhedra (EGFP-polyhedra) [4], and incubated for 72 h with activated recombinant MMP-1, -2, -3, -7, -8, -9, and -12. I subsequently measured the resulting fluorescence

(Figure 2-1A, Table 2-1). Significant release of intact fluorescent EGFP was observed with MMP-2 and MMP-8 but none of the other MMPs tested appeared to promote the release of intact, fluorescent EGFP. However, further experiments showed that substantial amounts of EGFP itself were degraded following incubation with two of the seven MMPs, MMP-3 and MMP-7, and it is therefore unknown whether these MMPs are able to degrade polyhedra (Figure 2-2, Table 2-2). MMP-2 and MMP-8 are classified as collagenases and gelatinases, respectively. Both enzymes, which are present in the connective tissue of most mammals, are known to be cleaving enzymes for tissues. These results suggest that these MMPs can be used for release of a cargo protein from polyhedra. On the other hand, when pEGFP were incubated with trypsin or chymotrypsin, significant release of intact EGFP was not observed. The reason was thought to be dependent on the presence of many sites in the EGFP molecule that are cleaved by trypsin and chymotrypsin (Table 2-3). I have concluded that an environment containing proteinases with a relatively high specificity for polyhedrin is required to obtain the release of intact, biologically active cargo proteins from polyhedra. I observed the change of the surface of polyhedra incubated with proteases (Figure 2-1C). It was confirmed that many pores are formed on the surface of polyhedra following protease treatment.

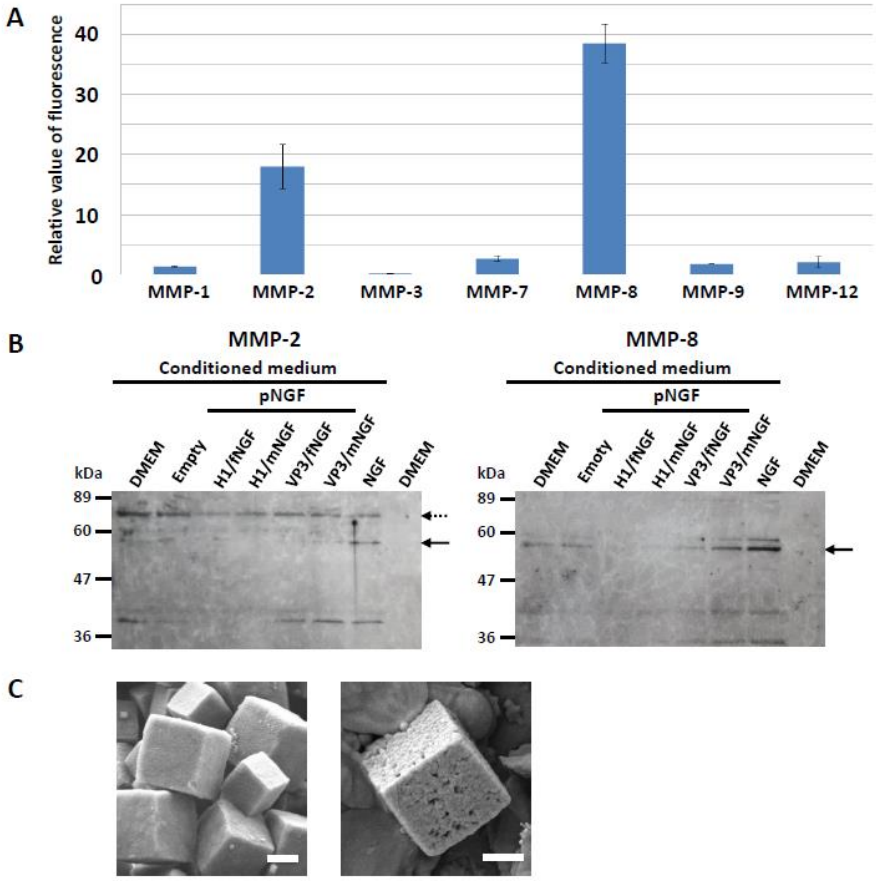

Figure 2-1. Release of cargo proteins by MMPs. (A) Analysis of proteins released from polyhedra. After H1-tagged pEGFP were incubated with MMP-1, -2, -3, -7, -8, -9, and -12 for 72 hr at 35 °C, the fluorescence of EGFP released from polyhedra was measured and shown as a relative value compared with a condition without each MMP. The relative fluorescence value is obtained by comparison with controls which were incubated without enzyme in Table 2-1. (B) Secretion of MMPs from PC12 cells. Cells were incubated in serum free medium (DMEM) containing each pNGF (NGF full-length (fNGF) and mature (mNGF) tagged with either H1 or VP3), empty polyhedra (Empty) and NGF-2.5S (NGF). Proteins secreted into the medium (conditioned medium) were subjected to SDS-PAGE and Western blot analysis by use of anti-MMP-2 (left) and anti-MMP-8 (right) antibody. The arrow and hatched arrow indicate active form and pro-form, respectively. The larger protein fragment (seen above the band indicated by the arrow in the MMP-8 panel) is likely derived from a single nucleotide polymorphism of MMP-8 gene [47]. Lower bands were also thought to be the degraded products of each MMP. (C) Polyhedra were purified (left, control) and subsequently incubated with proteases at 37 °C (right) and imaged with scanning electron microscopy (SEM). Scale bars, 1 μm.

Table 2-1. Fluorescence of EGFP released from polyhedra after incubation with MMPs. After pEGFP was incubated with each MMP for 72hr, EGFP released from polyhedra was measured. Mock was incubated without MMPs.

	Mean	SD
MMP-1	0.012	0.001
Mock	0.008	0.002
MMP-2	0.232	0.048
Mock	0.013	0.002
MMP-3	0.007	0.001
Mock	0.030	0.012
MMP-7	0.014	0.003
Mock	0.005	0.002
MMP-8	0.244	0.020
Mock	0.006	0.005
MMP-9	0.010	0.000
Mock	0.005	0.000
MMP-12	0.004	0.002
Mock	0.002	0.001

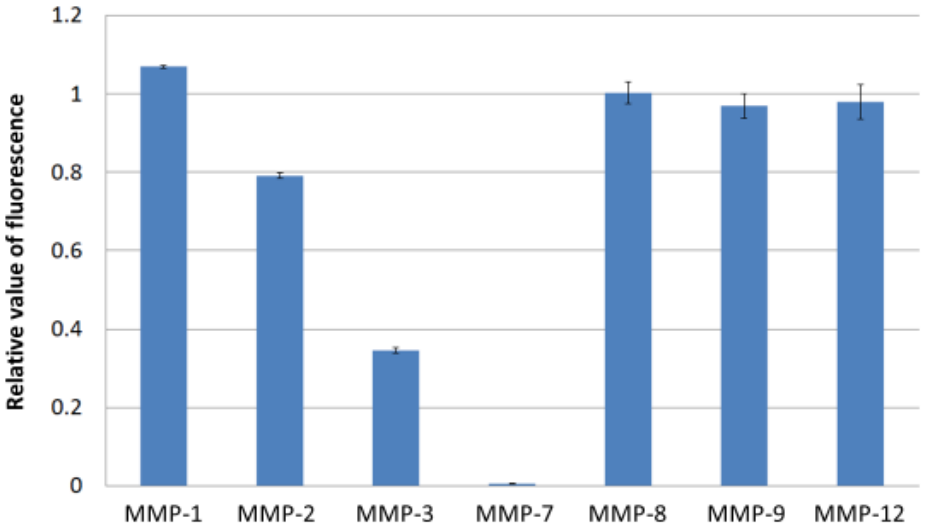

Figure 2-2. Effects of MMPs on EGFP. Recombinant EGFP was incubated with each MMP as indicated in 100 µl of TCNB buffer (5 mM Tris pH 7.5, 1 mM CaCl2, 15 mM NaCl, 0.005% Brij-35). After incubation at 35°C for 72 h, reactions were stopped by 12 µl of 0.5M EDTA (pH8.0) and supernatants were collected by centrifugation. Subsequently, fluorescence was measured in a plate reader (Ex/Em=485/538). Resulting values are plotted, normalized against a condition without each MMP (i.e. mock digest) set to 1.

Table 2-2. Fluorescence of soluble EGFP after incubation with MMPs. After soluble EGFP was incubated with each MMP for 72 hr, fluorescence was measured. Mock was incubated without MMPs.

	Mean	SD
MMP-1	4.58	0.02
Mock	4.28	0.01
MMP-2	1.81	0.02
Mock	2.29	0.10
MMP-3	0.78	0.02
Mock	2.27	0.21
MMP-7	0.18	0.00
Mock	3.34	0.02
MMP-8	1.07	0.03
Mock	1.07	0.00
MMP-9	4.14	0.13
Mock	4.27	0.21
MMP-12	5.12	0.23
Mock	5.22	0.12

Table 2-3. Fluorescence of EGFP after incubation with trypsin and chymotrypsin. After H1-tagged pEGFP (3.0×10^6 cubes /100 μl) were incubated with each 2 μg of trypsin and chymotrypsin for 12 hr at 37 °C, the fluorescence of EGFP released from polyhedra was measured.

Enzyme	**Fluorescence intensity (arbitrary units)**
Trypsin	0.12
Chymotrypsin	0.15
No enzyme	0.03

In order to confirm that MMPs from PC12 cells are a likely source of proteases that degrade polyhedra, the expression of MMPs by PC12 cells was studied using western blot analysis, reverse transcription PCR. Full-length NGF (fNGF) or mature NGF (mNGF) was fused with polyhedra-targeting tags (H1 or VP3) to obtain pNGF (pfNGF or pmNGF) (Figure 2-3A). PC12 cells were incubated in serum-free medium containing pfNGF and pmNGF tagged with either H1 or VP3, empty polyhedra and NGF-2.5S.

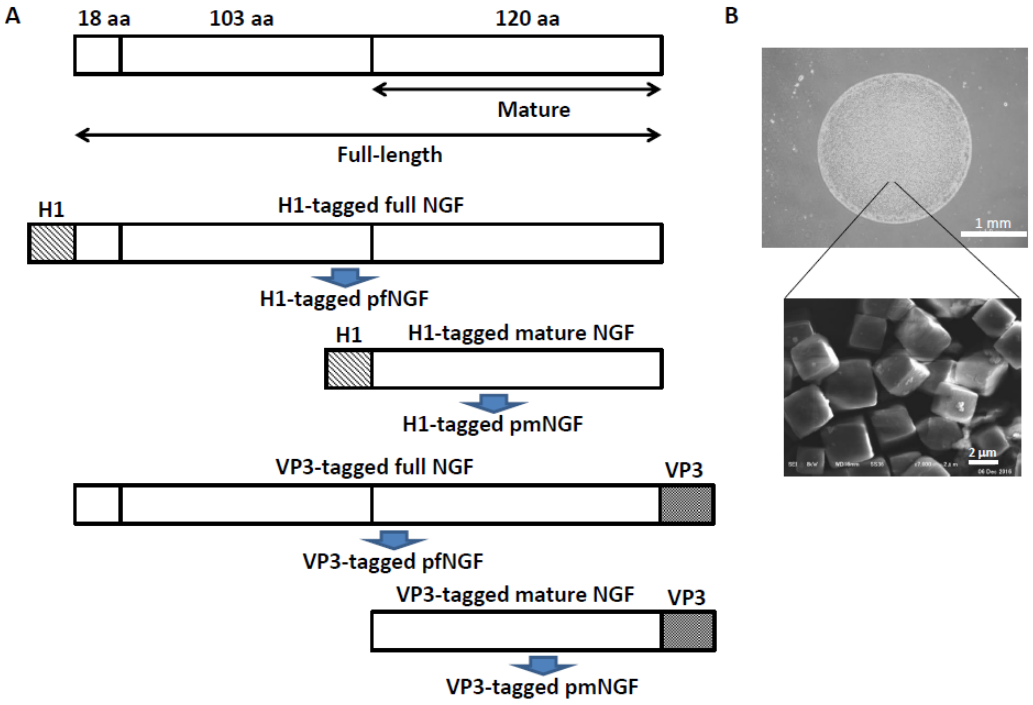

Figure 2-3. Construction and spotting of NGF-encapsulated polyhedra. (A) Full-length and mature NGF (fNGF and mNGF, respectively) were fused with either a H1 or VP3 tag, and each recombinant NGF fusion protein was encapsulated into polyhedra to make H1-tagged or VP3-tagged pfNGF and H1-tagged or VP3-tagged pmNGF, respectively. (B) Spot of pNGF and SEM image of pNGF.

Western blot analysis of the culture media showed that both MMP-2 and MMP-8 were indeed secreted into the medium by PC12 cells: both proteins could be detected in conditioned media across all culture conditions but not in non-conditioned medium (Figure 2-1B). I noted that MMP-2 and MMP-8 were secreted at similar levels to PC12 cells cultured with empty polyhedra and with medium only (Figure 2-1B), suggesting that secretion was not stimulated by either the polyhedrin protein or the released cargo protein NGF. This observation was also confirmed by investigating the levels of gene expression of MMPs in PC12 cells using RT-PCR (Figure 2-4). Although MMP-1 is produced by fibroblasts in a variety of connective tissues [48] and MMP-7 is mainly expressed in epithelial cells in endometrium, small intestine, breast, parotid, pancreas, liver, prostate, dermis, and bronchus [48], the expression of MMP-1 and MMP-7 in PC 12 cells was not detected by qPCR analysis.

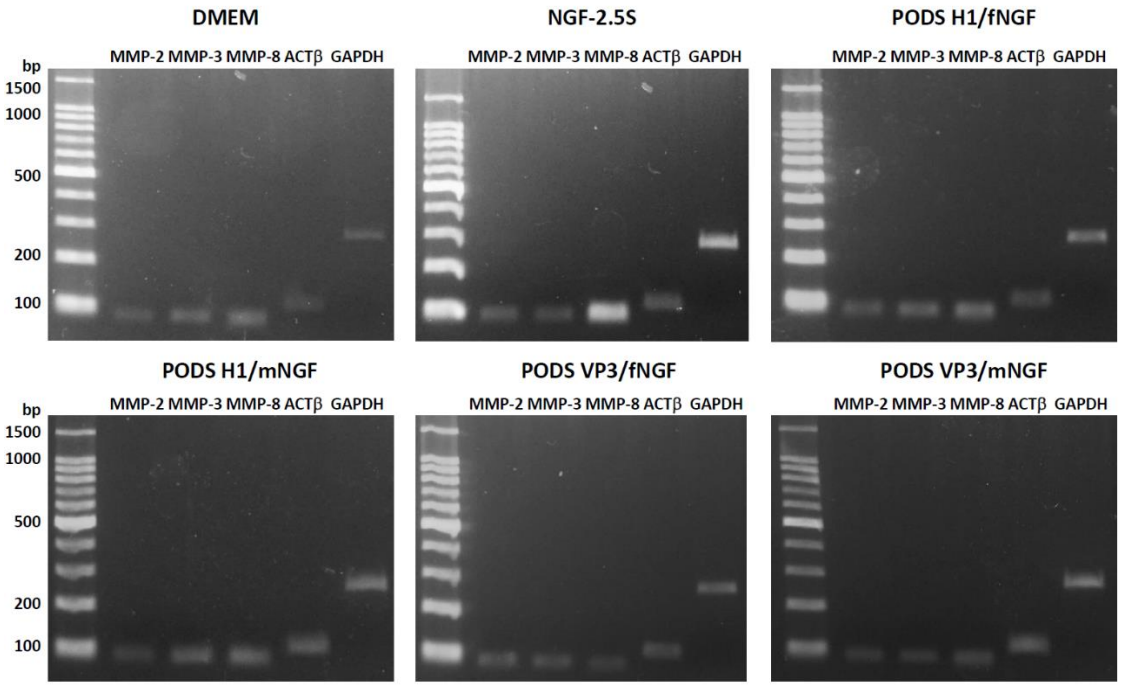

Figure 2-4. RT-PCR of MMP-2, -3, and -8 expression. PCR amplifications were performed by each number of cycles (34 for MMP-2, 36 for MMP-3, 40 for MMP-8). Housekeeping genes, actin β (ACTβ) and glyceraldehyde-3 phosphate dehydrogenase (GAPDH) were also amplified by 22 cycles.

Alignment of PC12 cells by pNGF.

One microliter of either a high or low concentration polyhedra suspension of either pfNGF or pmNGF (5×10^4 or 1×10^5 cubes /μl) was manually spotted onto a gelatin-coated coverslip using a micropipette to create a circular field approximately 2-4 mm in diameter (Figure 2-3B). PC12 cells were seeded across the coverslip and cultured with serum-free medium under static conditions for 5 days without any media changes. Both pfNGF and pmNGF prominently induced axon extension from each cell (Figure 2-5C to 2-5F). Surprisingly, this axon extension was parallel with the edge of the polyhedra field resulting in the formation of a connected chain of migrated cells (Figure 2-5G to 2-5M). In contrast, when PC12 cells were incubated with the conventional NGF-2.5S, axons were randomly extended from cells (Figure 2-5A). Furthermore, extension of axons was not observed for empty polyhedra, i.e. without encapsulated NGF (Figure 2-5B). Alignment and extension of axons from PC12 cells surrounding pfNGF and pmNGF fields was also observed using scanning electron microscopy (SEM) (Figure 2-5G to 2-5M).

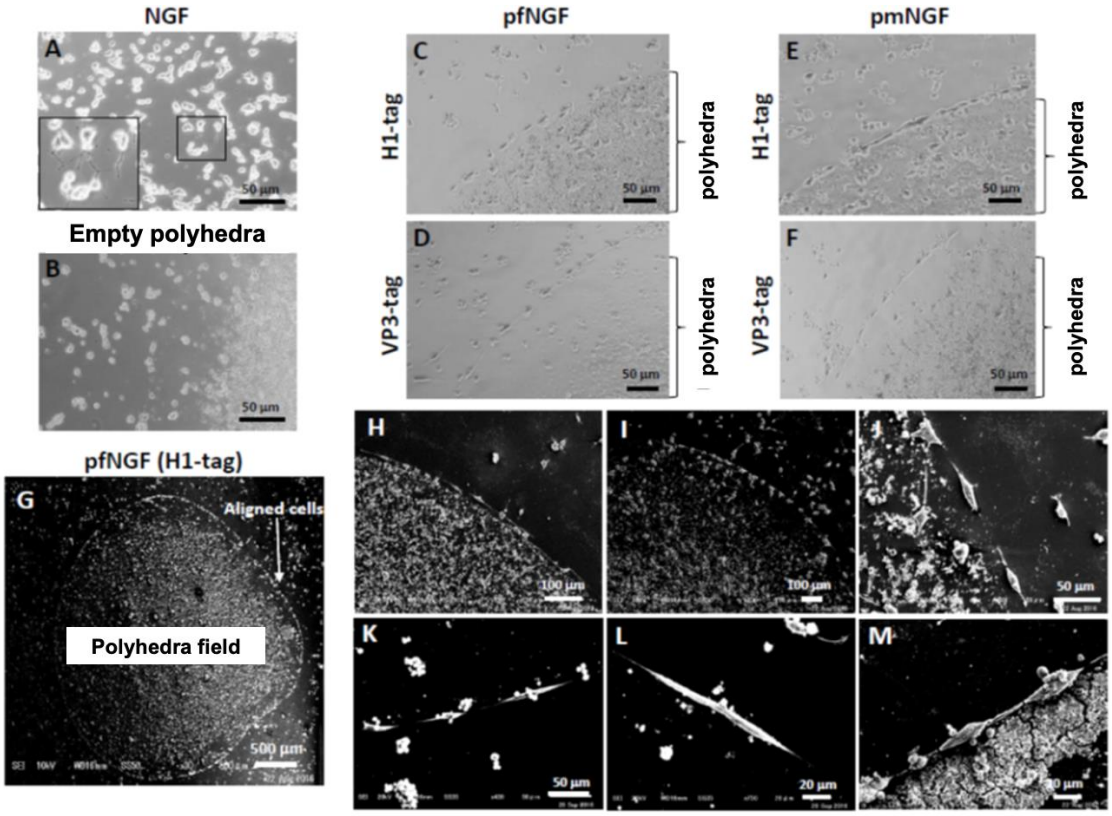

Figure 2-5. Alignment of PC12 cells surrounding the periphery of polyhedra field. PC12 cells were seeded and incubated with NGF-2.5S from the murine submaxillary gland (NGF) (A). The box is a magnified image to show randomly extended axons. After empty polyhedra (B) and H1-tagged pfNGF (C, G, H, J), H1-tagged pmNGF (E, I), VP3-tagged pfNGF (D, K, L, M), and VP3-tagged pmNGF (F) were spotted onto collagen-coated cover slips, PC12 cells were seeded and incubated for 5 days without medium exchange.

Differentiation of PC12 cells

I examined expression of tau, neurofilament, and GAP-43, which are neural differentiation markers (Figure 2-6). These differentiation markers were detected in the PC12 cells aligned by the pfNGF, but no signal was observed from PC12 cells incubated adjacent to empty polyhedra (Figure 2-6A). Notably, an intermediate filament protein neurofilament was also detected in the extended axon, indicating that the aligned cells are differentiated to nerve cells (Figure 2-6B). It is known that NGF induces not only the formation of growth cones in PC12 cells, but also another kind of neurite terminal structure, the varicone, which has a hybrid character of growth cone and varicosity [45]. Expression of GAP-43 was observed in some of the neurite termini of the extended axons from cells (Figure 2-6B). It is known that GAP-43 is concentrated in axonal growth cones but is not detected in growing dendrites and dendritic growth cones.

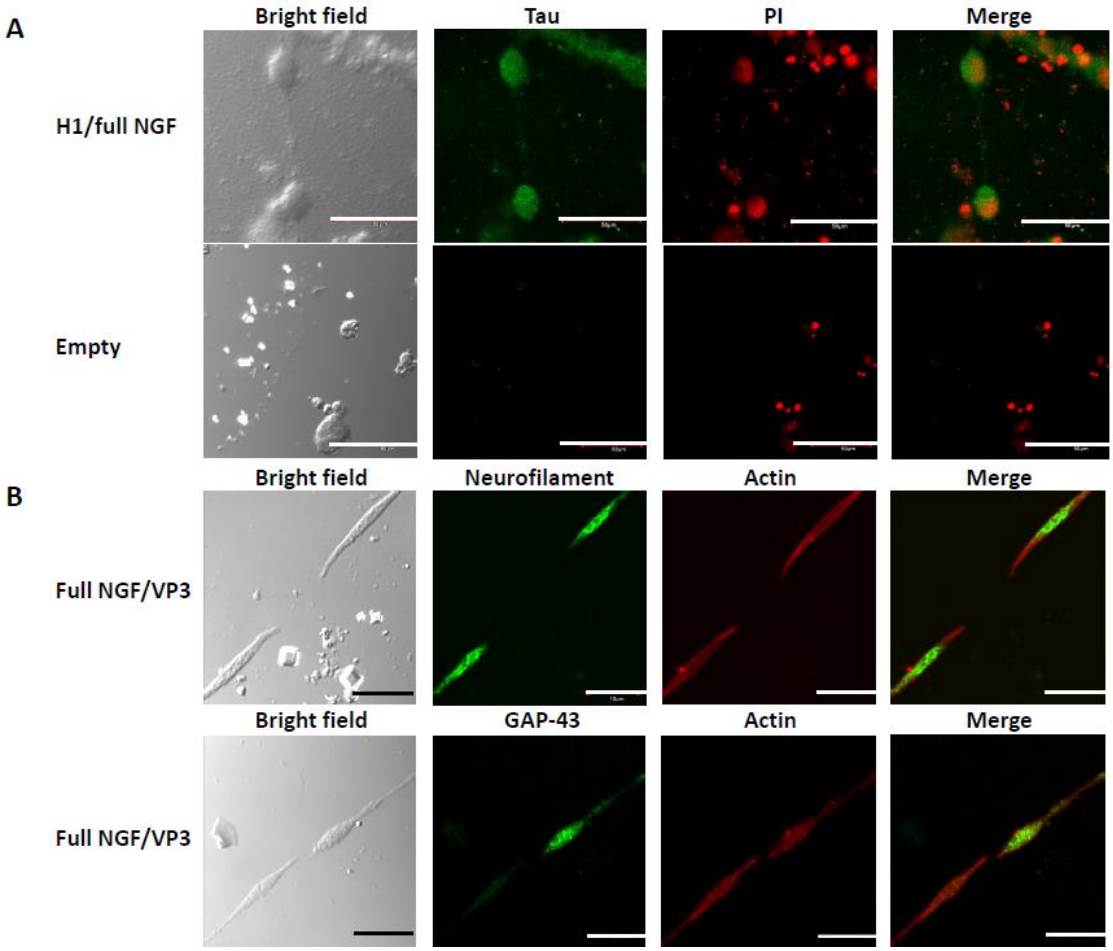

Figure 2-6. Expression of neural differential markers in the aligned PC12 cells. (A) Expression of tau. PC12 cells were incubated with H1-tagged pfNGF (H1/full NGF) or empty polyhedra (Empty). Expression of tau and nuclei were detected by immunofluorescence cytochemistry and propidium iodide (PI) staining. (B) Expression of neurofilament, GAP-43 and actin. PC12 cells were incubated with VP3-tagged pfNGF (Full NGF/VP3). Each protein was detected by immunofluorescence cytochemistry. Scale bars, 50 μm.

Connections between cells

In some cases, connections of the PC12 cells aligned by pfNGF were observed between the extended axon of one PC12 cell and the growth cone-like structure of an adjacent PC12 cell (solid box in Figure 2-7A). In other cases, the connection between PC-12 cells was less clear from neurofilament staining (dotted box in Figure 2-7A). Nonetheless, formation of connections between the neurite terminals was confirmed by the expression of a gap junction protein. Expression of connexin 43, a gap junction protein, was observed in connecting sections of the neurite terminals from aligned cells (Figure 2-7B). Additionally, extension of very fine filopodia from growth cones was observed by SEM and, interestingly, filopodia facing each other appear to be connected (Figure 2-7C). These results showed that pfNGF induced many types of structures on the neurite terminals of the extended axons from the aligned PC12 cells.

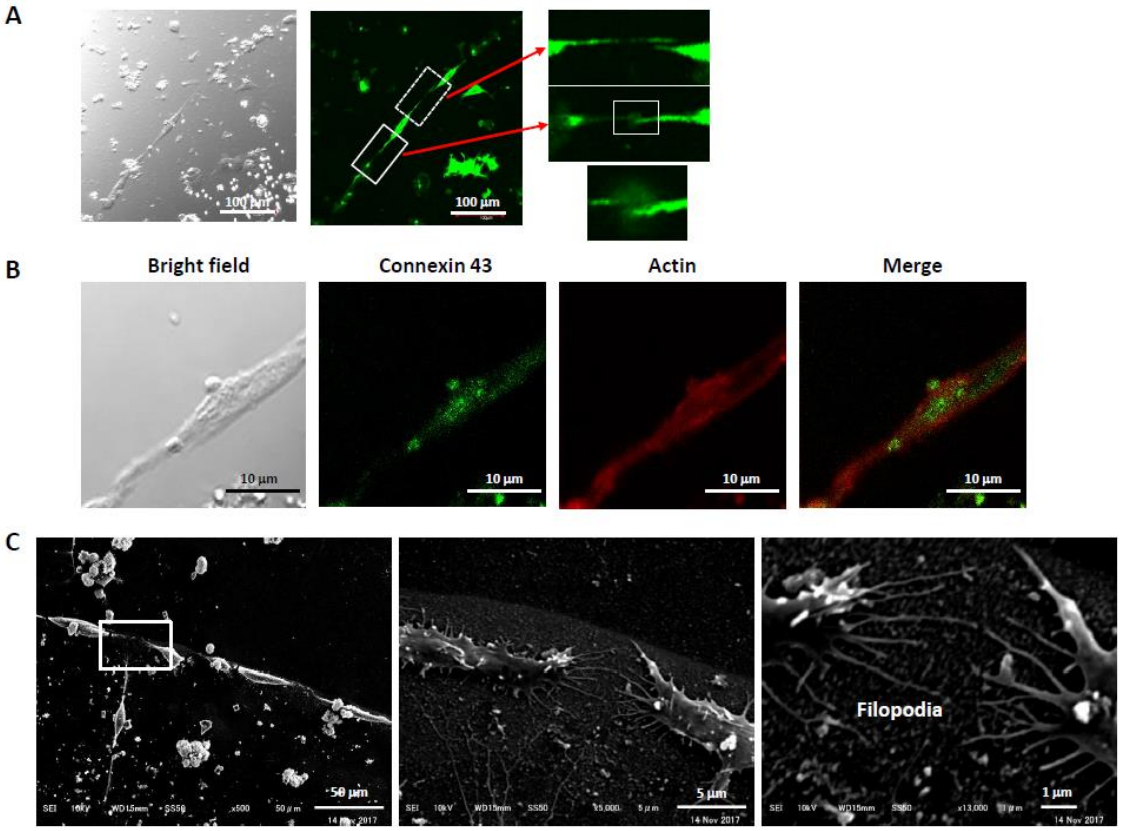

Figure 2-7. Connections between the aligned PC12 cells. (A) Connection via the extended axon. The extended axon induced by H1-tagged pfNGF was detected by expression of neurofilament. Connections between the extended axon and the growth cone-like structure (solid box) and between the axons (dotted box) were observed. (B) Expression of connexin 43. A gap junction protein connexin 43 was detected in connecting sections of the extended axons. (C) Connection by filopodia. Very fine filopodia were extended and connected between growth cones.

Discussion

NGF is an important neurotrophic factor responsible for the growth, differentiation, and survival of sympathetic and neural crest-derived sensory neurons. Although PC12 cells are immortalized and do not always behave in the same way as primary neuronal cells, stimulation of pheochromocytoma PC12 cells by NGF leads to growth arrest and neuronal differentiation. In the presence of NGF, PC12 cells also differentiate into sympathetic-like neurons [49]. Furthermore, NGF promotes microtubule assembly thereby regulating neurite formation during neuronal differentiation [50], and NGF-treated PC12 cells exhibit many of the hallmarks of differentiated neurons. These characteristics combine to make PC12 cells a useful model for studying neuronal differentiation and neurite outgrowth.

In the cell cultures, I observed PC12 cells forming a single chain around the pNGF field with a distinct zone on the periphery of this region which is devoid of cells. I also showed that pNGF-induced differentiation to neural cells with a variety of neurite terminal and connection via axons, growth cones and filopodia. These axonal connections were also perpendicular to pNGF field allowing the PC12 cells to form a single, unbranched chain. I speculate that the PC12 cells in the chain are producing an inhibitor

that prevents additional PC12 cells from migrating up along the pNGF field and joining the structure.

Polyhedra have the ability to release proteins over long periods of time but are eventually degraded. This is important for therapeutic applications. In the previous study [12], bone morphogenetic protein-2 (BMP-2)-encapsulated polyhedra (pBMP-2) were implanted with an absorbable collagen sponge (ACS) in critical-sized bone defects. This resulted in near-complete bone healing at 15 weeks following implantation. Many polyhedra remained intact with the ACS 5 weeks after implantation, but were not visible, being entirely replaced with newly generated bone, at 15 weeks. Although we tested the *in vivo* implantation of three other polyhedra in addition to pBMP-2 [6, 42, 43], there was no evidence of inflammatory or foreign-body reaction from the host tissues adjacent to the implantation of polyhedra.

It is important to understand the mechanism by which polyhedra release their cargo. In this study, I showed that EGFP cargo protein in polyhedra was released by MMP-2 and MMP-8. As it was confirmed that PC12 cells expressed and secreted MMP-2 and MMP-8, I conclude that the gradient of NGF was formed consequent to the secretion of these proteases by PC12 cells.

Release of intact cargo protein requires degradation of surrounding polyhedrin protein. This process will be more efficient if the cargo protein is more resistant to MMPs. This may be expected given the different origins of the proteins: Not withstanding their typically short half-lives, growth factors have evolved to function in the metalloprotease-rich environment of the ECM. In contrast, polyhedrin protein has evolved to maintain integrity in external environments (such as foliage surfaces) which do not require resistance to MMPs. Therefore, polyhedrin may be inherently more susceptible to MMPs enabling intact release of MMP-resistant cargo proteins and functionality of the polyhedra.

NGF promotes neurite outgrowth. When NGF-2.5S is homogenously distributed in the medium, PC12 cells randomly extended axons (Figure 2-5). However, when localized pNGF fields were created, the appearance of PC12 cells was radically altered compared with appearance in the presence of soluble NGF-2.5S (Figure 2-5G). It has been shown previously that proteins are slowly released from polyhedra [10]. The resulting microenvironment resulted in the induction of differentiation and alignment of PC12 cells.

When a gap is less than 5 mm, a common strategy for peripheral nerve injuries is to join the distal and proximal stumps of the damaged nerves by microsurgery. When the gap is longer than 5 mm, direct microsurgery generates tension in the nerve fibers.

Therefore, a nerve graft is required to fill the gap and make the connections between the distal and proximal stumps of the damaged nerves. I have already shown that neural cells are aligned along the periphery of a pNGF field with a diameter of about 2 to 5 mm (Figure 2-3B and Figure 2-5G). I estimate that my current methods will allow for the generation of about 6 to 15 mm nerve fibers for nerve grafts into an injured nerve. Although the side effects by the implantation of polyhedra were not observed in the previous study [12, 51, 52], further experiments will be needed to elucidate utility for the repair or regeneration of nerve fiber *in vivo*.

Chapter 3

Effects of transgenic silk materials that incorporate FGF-7 protein microcrystals on the proliferation and differentiation of human keratinocytes

Introduction

The middle silk gland (MSG) and posterior silk gland (PSG) of silkworms, *Bombyx mori*, produce large quantities of silk thread proteins [17]. Recombinant versions of proteins produced in these MSGs [Publication List 3, 12-14] and PSGs [8, 20, 21, 53] are used in protein engineering. The PSG expresses the biopolymer protein fibroin, which is highly biodegradable, biocompatible, and shows low immunostimulatory activity, making it suitable to produce surgical sutures [20] and grafts for revascularization [22], and for bone tissue regeneration [23] and cutaneous wound healing [24, 54].

Posterior silk glands engineered to express cell growth factors could be processed into biomedical materials, such as powders with high concentrations of fibroin, which could control the proliferation of cells *in vivo* and *in vitro.* However, one potential disadvantage of this system is that cell growth factors, including the human fibroblast growth factor-7 (FGF-7), are typically unstable under harsh environmental conditions, causing them to have a short half-life [3, 55].

The *B. mori* cypovirus 1 (CPV), which is a member of the family *Reoviridae*, produces proteinaceous occlusion bodies known as polyhedra that include microcrystals of the protein polyhedrin, which has attracted attention for its potential ability to encapsulate and protect proteins [3-6]. This virus infects cells in the silkworm digestive

tract, producing large numbers of polyhedra. Progeny viruses are occluded in polyhedra that protect against infectivity over the long-term and in the outdoor environment [3]. Previous study showed that polyhedra could encapsulate diverse foreign proteins, such as fluorescence proteins [4-7], cytokines [Publication List 1, 8-10], and fusion proteins comprising enzymes [11] with an N-terminal polyhedron-targeting signal alpha-helix sequence H1 and C-terminal VP3-tag that are expressed during polyhedron crystallization in cultured insect cells. In addition, the cytokine activities in polyhedra are stable in the long-term [4]. The remarkable stability of polyhedra-encapsulated proteins suggests that these systems could be robust as sustained-release carriers of cytokines and other proteins for tissue engineering [Publication List 1, 4, 8-11].

I also recently reported that the introduction of polyhedra into an *in vitro* neurodifferentiation cell culture model induced the release of active neutrophin from polyhedra upon gradual polyhedra proteolysis mediated by small amounts of cell-derived matrix metalloproteinases [Publication List 1]. These findings highlight the potential biomedical applications of polyhedra that encapsulate cytokines, such as FGF-7, inside silkworm silk glands. These silk glands can be processed to yield silk materials incorporating cytokine-polyhedra to control cell proliferation.

The earlier studies showed that protein expression systems involving

bioengineered silk glands could effectively produce active cytokines, such as fibroblast growth factor-2 (FGF-2; ref. 16). Here, I focused on the generation of transgenic silkworms using PSGs and MSGs that produce polyhedron-encapsulated FGF-7 (pFGF-7). FGF-7 is used for establishment of a three-dimensional (3D) culture system that serves as an *in vitro* model epidermis [25]. I examined whether the biological activity of FGF-7 can be released from the polyhedra to induce keratinocyte proliferation and epidermal differentiation of cells in supplement-free culture. I also investigated the effectiveness of FGF-7 activity released from polyhedra that are incorporated in PSGs in 3D keratinocyte cultures to inform the construction of a human epidermis model.

MATERIALS AND METHODS

Silkworms

Non-diapausing *w1-pnd* lines that lay non-pigmented eggs were used to generate transgenic silkworms [56]. Silkworm larvae were aseptically reared at 25°C on an artificial diet (Aseptic Sericulture System Laboratory, Kyoto, Japan).

Cultured cells

Normal human epidermal keratinocytes (NHEKs; Kurabo, Osaka, Japan) were cultured using Humedia KG-2 medium (Kurabo) supplemented with insulin (10 μg/ml), human EGF (0.1 ng/ml), hydrocortisone (0.67 μg/ml), gentamycin (50 μg/ml), amphotericin (50 ng/ml), and bovine pituitary extract (0.4% V/V) in 5% CO_2 at 37°C. Keratinocytes in the third passage were cultured using a defined keratinocyte-serum free medium (DK-SFM) supplemented with defined keratinocyte-SFM growth supplement that included insulin, EGF, and FGF (Thermo Fisher Scientific, Waltham, MA, USA).

Plasmid construction and microinjection

A FGF-7 sequence fused with an H1-tag (H1/FGF-7) and *Nhe*I sites at both ends was amplified using polymerase chain reaction with the primers 5′-

AAAGCTAGCATGGCAGACGAGCAG-3′ (forward) and 5′-AAAGCTAGCTTAAGTTATTGCCTAGGAAG-3′ (reverse) and a vector previously used for the construction of recombinant FGF-7-expressing baculovirus as the template to construct donor plasmids for transgenesis [4]. The amplified fragments were digested with *Nhe*I and inserted into the *Bln*I site downstream of the upstream activation sequence (UAS) in the pBacMCS[UAS/SV40,3×P3-enhanced green fluorescent protein (EGFP)] plasmid [57]. The resulting plasmid, pBacMCS[UAS-H1FGF-7/SV40,3×P3-EGFP], was purified from the bacterial culture using QIAGEN Midi (Qiagen, Hilden, Germany).

To generate transgenic silkworms that expressed H1/FGF-7 in their silk glands, I performed microinjection as previously described [58]. I observed EGFP present in the eyes in G1 eggs using fluorescence microscopy with an Olympus IX71 light microscope (Olympus, Tokyo, Japan). The transgenic line carrying the gene for H1/FGF-7 (UAS-H1/FGF-7 line) was established through repeated sibling mating of selected individuals exhibiting EGFP expression in the eyes.

Genomic DNA was isolated from the UAS-H1/FGF-7 line, and the sequences at the borders of the transgene insertion were assessed using inverse PCR, and database analysis was conducted using the KAIKOBLAST database (*http://kaikoblast.dna.affrc.go.jp*). DNA was digested with *Sau*3A1 (Takara Bio Inc.,

Shiga, Japan) and circulated using Ligation High ver.2 (Takara Bio Inc.). The ligated DNA was amplified using KOD plus version 2 DNA polymerase (Toyobo, Osaka, Japan) under standard conditions with primers designed based on the left- and right- hand region of the vector (left primer pair, 5′-GCGTGAGTCAAAATGACGCATGAT-3′ and 5′-ATCAGTGACACTTACCGCATTGACA-3′ and right primer pair, 5′-CCTCGATATACAGACCGATAAAACAC-3′ and 5′-AACTTTTATGGCGCGCCATCGAAT-3′). The purified fragments were sequenced directly (ABI PRISM® 310 Genetic Analyzer, Applied Biosystems, Foster City, CA, USA) using primers for the left (5′-GACTGAGATGTCCTAAATGCACAG-3′) and right boundary (5′-GACCGATAAACACATGCG-3′) of the vector.

Generation of transgenic silkworms that express H1/FGF-7 and polyhedra

The UAS-H1/FGF-7 line was mated with PSG- (FH-GAL4; ref. 39) or MSG-specific (S1-GAL4; ref. 40) Gal4 driver lines to obtain FH-H1/FGF-7 (Figure 3-1B) or S1-H1/FGF-7 lines (Figure 3-4A) expressing H1/FGF-7 under the control of the fibroin heavy chain gene (*FH*) promoter in PSGs or the Sericin 1 gene (*SI*) promoter in MSGs. Both promoters are active during the larval spinning stage [59, 60]. The transgenic line carrying CPV polyhedrin (UAS-polyhedrin line; ref. 7) was then mated with the FH-

GAL4 or S1-GAL4 line to obtain an FH-polyhedrin line expressing polyhedrin in PSGs (Figure 3-1C) or S1-polyhedrin in MSGs (Figure 3-4B). Finally, the UAS-H1/FGF-7 line was mated with the FH-polyhedrin line to obtain the FH-poly/H1/FGF-7 line (Figure 3-1C), which expresses both H1/FGF-7 and polyhedrin in PSGs under control of the *FH* promoter. The S1-polyhedrin and UAS-H1/FGF-7 lines were mated in the same way to obtain the S1-poly/H1/FGF-7 line (Figure 3-4B), which expressed both H1/FGF-7 and polyhedrin in MSGs under the control of the *S1* promoter.

H1/FGF-7 immunoblotting

H1/FGF-7 was purified from the PSG of larvae of the FH-H1/FGF-7 line at the spinning stage by immunoprecipitation using a Dynabeads Protein A kit (Thermo Fisher Scientific) following the manufacturer's instructions. A measure of 50 mg of PSGs from FH-H1FGF-7 or *w1-pnd* control larvae were dissolved in RIPA buffer (Nacalai Tesque, Kyoto, Japan) using sonication. After centrifugation at 6,000 × g for 5 min, the supernatants were incubated with protein A Dynabeads bound to an anti-FGF-7 antibody (ReliaTech GmbH, Wolfenbüttel, Germany) overnight at 4°C. Dynabead-Ab-Ag complexes were washed with the washing buffer supplied in the kit and then lysed in a sample buffer for immunoblotting. Fifty-thousand cubes of empty polyhedra with no H1/FGF-7 and pFGF-

7 [4] produced in baculovirus-infected Sf21 cell lines were used as negative and positive controls, respectively. Proteins in the samples were separated by 12.5% SDS-PAGE, transferred onto PVDF membranes (GE Healthcare Bioscience, Piscataway, NJ, USA) and blocked with Blocking One (Nacalai Tesque). After blocking, membranes were incubated in a primary antibody solution containing 1:5,000 anti-FGF-7 antibody, washed in PBS (−), and incubated in a secondary antibody solution containing 1:5,000 goat anti-rabbit IgG conjugated with horseradish peroxidase (Bio-Rad, Hercules, CA, USA). Target protein bands were visualized after incubation with detection reagent (GE Healthcare Bioscience).

The MSGs from S1-H1/FGF-7 larvae were examined in the same way using the abovementioned immunoblotting procedure.

Immunofluorescence of polyhedra from posterior or middle silk glands

Anti-Human FGF-7 was directly labeled with HiLyter Fluor^{TM} 555 following the manufacturer's instructions (HiLyter Fluor^{TM} 555 Labeling Kit-NH_2, Dojindo Laboratories, Kumamoto, Japan). Polyhedra from silk gland powders (SGPs) suspended in PBS (–) were collected using sonication and centrifugation. Polyhedra of PSGs from FH-poly/H1/FGF-7 or FH-polyhedrin larvae at the spinning stage were placed on the

bottom of glass-based dishes (Iwaki glass, Shizuoka, Japan). After air drying, polyhedra were blocked with Blocking One solution and incubated in a primary antibody solution containing anti-polyhedrin antibody diluted 1:1,000 and then washed in PBS (–) at room temperature for 15 min. After washing, polyhedra were further incubated in a secondary antibody solution containing 1:500 Alexa Fluor 488-conjugated anti-rabbit IgG (Invitrogen, Carlsbad, CA, USA). Then, they were washed in PBS (–). Next, the polyhedra were incubated in an antibody solution containing HiLyter Fluor^{TM} 555-labeled anti-FGF-7 antibody diluted 1:500, washed in PBS (−), and examined using an Olympus Fluoview FV1000-IX81 confocal microscope (Olympus) with a 100x objective lens. The MSG polyhedra from S1-poly/H1/FGF-7 or S1-polyhedrin larvae were examined with an anti-FGF-7 antibody, as described above.

Enzyme-linked immunosorbent assay analysis of H1/FGF-7 released from silk gland materials

The amount of H1/FGF-7 released from FH-poly/H1/FGF-7 larvae PSGs was determined using an enzyme-linked immunosorbent assay (ELISA) using an anti-FGF-7 antibody. The PSGs from spinning larvae of *w1-pnd* and FH-poly/H1/FGF-7 were freeze-dried and crushed into fine powders, which were called posterior silk gland powders (PSGPs).

Empty polyhedra and pFGF-7 were prepared using similar methods to those described by Ijiri *et al.* (2009) in the recombinant baculovirus-infected *Spodoptera frugiperda* cells (Sf21 cells). Keratinocyte-conditioned medium (KCM) was harvested from NHEKs cultured (3.0×10^4 cells /ml) in DK-SFM without a growth supplement for 48 hr. Over 14 days, 5.0×10^5 cubes of polyhedra and 1 mg of PSGPs were added to KCM using a cell culture insert filter. Media were collected on days 3, 7, 10, and 14, and the quantity of FGF-7 in the collected culture medium was determined using a Human KGF/FGF-7 Quantikine ELISA kit (R&D Systems, Minneapolis, MN, USA), following the manufacturer's instructions. The amount of soluble H1/FGF-7 was quantified by measuring the absorbance at 450 nm with a microplate reader (Bio-Rad Model 680, Bio-Rad). Media incubated with empty polyhedra or PSGPs prepared from *w1-pnd* larvae were used as blanks for the ELISA analysis for the media incubated with pFGF-7 or PSGP from FH-poly/H1/FGF-7 larvae, respectively.

Detection of phosphorylation of p44/p42 mitogen-activated protein kinase

The PSGPs from FH-polyhedrin, FH-H1/FGF-7, and FH-poly/H1/FGF-7 spinning larvae and middle silk gland powders (MSGPs) from S1-polyhedrin, S1-H1/FGF-7, and S1-poly/H1/FGF-7 spinning larvae were obtained as described above. Then, these PSGPs

and MSGPs were stored at −80°C until use.

NHEKs were seeded onto six-well tissue culture plates (Iwaki glass) at 2.5×10^4 cells/well and cultured to confluence in Humedia KG-2 media for four days. After incubation, the medium was replaced with Humedia KB-2 medium (Kurabo) lacking growth supplement and incubated for 16 hr to induce starvation. After starvation, a cell culture insert (Corning, Corning, NY, USA) was placed in the well, and 10 mg of PSGPs or MSGPs from a series of silkworms were suspended in Humediua KB-2 and added onto the filter of each cell culture insert. Recombinant human FGF-7 (rhFGF-7; 100 ng/ml; Wako Chemical, Tokyo, Japan) was added as a positive control. Cells were incubated with PSGPs or MSGPs for 1 hr, washed with HEPES buffer (Kurabo), and dissolved in 100 µl SDS-PAGE sample buffer (50 mM Tris-HCl, pH 6.8, 100 mM dithiothreitol, 2.0% SDS, 0.1% bromophenol blue, 10% glycerol). Each cell lysate was analyzed using immunoblotting as described above, with Phospho-p44/p42 MAP Kinase (Thr202/Tyr204) antibody (1:2,500; Cell Signaling Technology, Danvers, MA, USA) or p44/p42 MAP Kinase antibody (1:5,000; Cell Signaling Technology) as the primary antibody. Protein bands were detected using an HRP-conjugated anti-rabbit IgG (1:5,000, Bio-Rad).

Assay for keratinocyte proliferation

To measure NHEK proliferation, we used a Cell Counting Kit-8 (CCK-8, Dojindo Laboratories), which detects intracellular dehydrogenase using water-soluble tetrazolium salt WST-8. NHEKs were seeded at 5×10^3 cells/well onto 24-well culture plates (Iwaki glass) in DK-SFM without growth supplement. Cell culture inserts were placed in the well, and suspensions of PSGPs (50, 100, or 200 μg) or MSGPs (50, 250, or 500 μg) in DK-SFM were added onto the filter of each cell culture insert. rhFGF-7 (2, 4, or 10 ng/ml) was used as a positive control. After culturing for 72 hr at 37°C in 5% CO_2, 10% (v/v) CCK-8 was added to the medium and incubated for 2 hr at 37°C under 5% CO_2. The absorbance of media was then measured at 450 nm using a microplate reader.

3D culture of keratinocytes

For 3D cultures, 800 μg PSGPs from FH-polyhedrin or FH-poly/H1/FGF-7 larvae were mixed in 250 μL of collagen solution (Cellmatrix Type I-A; Nitta Gelatin Inc, Osaka, Japan). The gelated collagen was poured into a RING-12 cloning ring (φ10 mm; Iwaki glass) in a six-well plate and incubated for 1 hr at 37°C in 5% CO_2. In this experiment, DK-SFM was used as a basal medium without growth supplement, and basal medium mixed with 1.2 mM Ca^{2+} was used as a differentiation medium. A measure of 4 mL of

basal medium was added to each well, and then 2.0×10^5 NHEKs suspended in 200 μL of basal medium were deposited on a collagen gel. After the NHEKs were submerged in the basal media for two days, the cloning rings were removed, and the basal medium was discarded. Then, 1 ml of the differentiation medium was added into each composite culture, and it was raised to the air-liquid interface for 14 days. Each differentiation medium was replaced twice weekly. 3D cultures of keratinocytes on the gel were also incubated with basal and differentiation media containing 100 ng/mL rhFGF-7.

After 14 days, the 3D keratinocyte cultures were fixed in 4% formaldehyde overnight. The fixed 3D cultures were then embedded in optimal cutting temperature compound (Sakura Finetek Japan, Tokyo, Japan) and cut into 20 micron-thick sections, which were placed on glass slides. The sections were hydrated and stained with hematoxylin and eosin (HE) before observing them with a light microscope (Olympus IX71, Olympus) with a 40× objective lens. For immunohistochemistry, sections were incubated with primary antibodies for keratin 14 (Invitrogen), keratin 10 (Abcam, Cambridge, United Kingdom), loricrin (BioLegend, San Diego, CA), and filaggrin (Santa Cruz Biotechnology, Dallas, TX). After washing in PBS(−), sections were incubated with Alexa Fluor 488-conjugated anti-rabbit IgG (Invitrogen) or Alexa Fluor 594-conjugated anti-mouse IgG (Invitrogen). Then, the nuclei were stained with 4′,6-diamidino-2-

phenylindole. Immunofluorescence imaging of the sections was conducted using confocal microscopy with a 40× objective lens.

Data analysis

All results are expressed as the mean ± standard deviation (SD) of triplicate assays (N = 3 independent samples). Data were analyzed using a one-way analysis of variance followed by Tukey's posthoc test for pair-wise comparisons. Differences were considered to be significant at $P < 0.05$ and $P < 0.01$.

RESULTS

Establishment of transgenic silkworms expressing H1/FGF-7 in posterior silk glands

I first analyzed the expression of FGF-7 with an N-terminal polyhedron-encapsulation signal H1 (H1/FGF-7; ref. 2) in the silk glands of transgenic silkworms. A donor plasmid (Figure 3-1A) was used for transgenesis of the silkworms and to establish a UAS-H1/FGF-7 line carrying the transgene. The presence of the transgene in chromosome 8 of the UAS-H1/FGF-7 line was confirmed using inverse PCR (Table 3-1). The FH-H1/FGF-7 line was generated by mating the UAS-H1/FGF-7 line with an FH-GAL4 line [59] carrying the GAL4 gene under the control of the *FH* promoter (Figure 3-1B). Immunoprecipitation with an anti-FGF-7 antibody was performed to examine PSG samples from the FH-H1/FGF-7 line in the spinning stage (Figure 3-2). Neither the negative control sample of recombinant baculovirus-produced empty CPV polyhedra in Sf21 cell lines (lane 1) nor immunoprecipitated proteins of PSGs in *w1-pnd* larvae (lane 3) showed bands for H1/FGF-7 in immunoprecipitation. In contrast, PSG proteins immunoprecipitated from FH-H1/FGF-7 larvae (lane 4) showed signals for H1/FGF-7 expression (calculated molecular mass ~24 kDa) as did the positive control sample of recombinant, baculovirus-produced polyhedra encapsulating H1/FGF-7 as previously described (lane 2; ref. 2).

The FH-poly/H1/FGF-7 line was generated by mating the UAS-H1/FGF-7 line with the FH-polyhedrin line that was previously shown to produce polyhedra in the PSG (Figure 3-1C; ref.10). Polyhedra (50,000 cubes) were collected from PSGs of FH-poly/H1/FGF-7 larvae at the spinning stage and analyzed using immunoblotting with an anti-FGF-7 antibody (Figure 3-3A). The same number of polyhedra in PSGs from FH-polyhedrin larvae were analyzed in the same way as a negative control, and no H1/FGF-7 was detected (Figure 3-3A, lane 1). Together, these results demonstrate that H1/FGF-7 is present in polyhedra from FH-poly/H1/FGF-7 larvae (Figure 3-3A, lane 2).

Using immunofluorescence with anti-FGF-7 and anti-polyhedrin antibodies to examine the association of H1/FGF-7 with polyhedra in PSG collected from FH-poly/H1/FGF-7 larvae, I detected fluorescent anti-FGF-7 signals and anti-polyhedrin signals on the surface of polyhedra from FH-poly/H1/FGF-7 line PSGs (Figure 3-3B). This result is consistent with that of Ijiri *et al.* (2009), who detected fluorescent proteins with N-terminal H1 inside recombinant baculovirus-produced polyhedra [4], and thereby demonstrated that H1-fused foreign proteins were present inside of polyhedra due to H1 associating with the polyhedrin groove domain consisting of tyrosine cluster to tightly link the polyhedrin to each other during polyhedron crystallization. I only found an antibody signal at the surface (Figure 3-3B), even though H1/FGF-7 was present inside

the polyhedra. This is because the FGF-7 antibody could not enter into the polyhedra. These results suggested that expressed H1/FGF-7 was encapsulated into the polyhedra in the PSGs of FH-poly/H1/FGF-7 larvae.

The UAS-H1/FGF-7 line was mated with an S1-GAL4 line to produce the S1-H1/FGF-7 line that expressed Gal4 under the control of the *S1* promoter to generate a transgenic silkworm expressing H1/FGF-7 in MSGs (Figure 3-4A). I confirmed H1/FGF-7 expression in MSGs from S1-H1/FGF-7 spinning larvae using immunoblotting with the anti-FGF-7 antibody (Figure 3-4C). The UAS-H1/FGF-7 line was then mated with the S1-polyhedrin line to obtain transgenic S1-poly/H1/FGF-7 worms that express FGF-7 and polyhedra in MSGs at the spinning stage (Figure 3-4B). Immunofluorescence analysis showed that an anti-FGF-7 signal could be detected on the surface of polyhedra collected from MSGs of S1-poly/H1/FGF-7 larvae, but not on polyhedra from S1-polyhedrin larvae MSGs (Figure 3-4D). Restriction of H1/FGF-7 fluorescence to the polyhedra surface was likely due to the inability of the antibody to enter the polyhedra. These results suggest that MSGs of S1-poly/H1/FGF-7 larvae produced polyhedra that encapsulated H1/FGF-7.

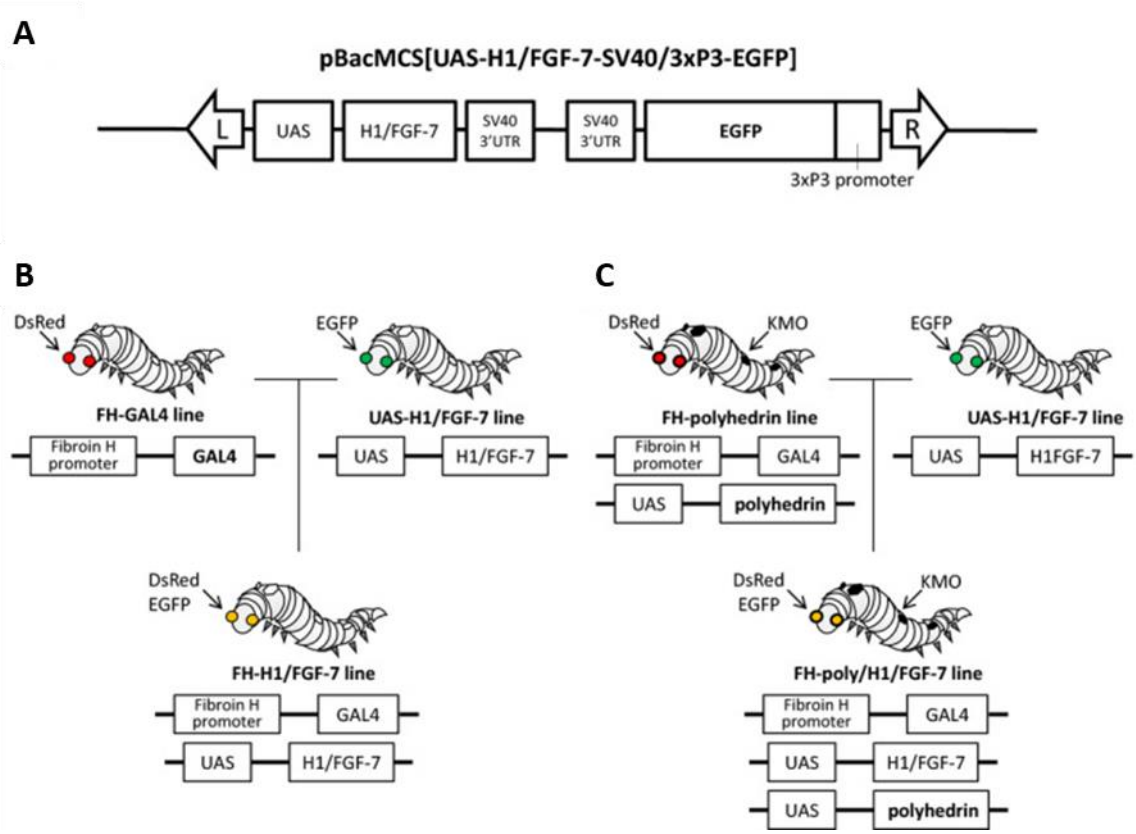

Figure 3-1. Generation of transgenic silkworms that express H1/FGF-7 in the posterior silk gland. (A) Schematic representation of the plasmid vector used to generate transgenic silkworms. The plasmid vector pBacMCS[UAS-H1/FGF-7-SV40/3xP3-EGFP] encoding H1/FGF-7 was used to generate the transgenic line termed UAS-H1/FGF-7. The *piggyBac* right and left inverted terminal repeats (ITRs) (L and R) are indicated by arrows. (B) Generation of the FH-H1/FGF-7 line. The FH-GAL4 line [59] was mated with the UAS-H1/FGF-7 line to generate the FH-H1/FGF-7 line in which expression of EGFP and discosome sp. Red (DsRed) as genetic markers is visible in the eyes. (C) Generation of the FH-poly/H1/FGF-7 line. The FH-polyhedrin line was mated with the UAS-H1/FGF-7 line to generate the FH-poly/H1/FGF-7 line with the expression of EGFP and DsRed visible in the eyes and kynurenine 3-monooxygenase (KMO) specific expression in the skin [16], as genetic markers.

Table 3-1. Inverse PCR of the UAS-H1/FGF-7 transgene border sequence in the *w1-pnd* genome and sequence analysis with the Kaikoblast database (http://kaikoblast.dna.affrc.go.jp). The chromosome number and clone name are listed for the border sequence. The TTAA consensus sequence appearing at the border of the *piggyback*-driven transgene is underlined.

Silkworm line	Sequence at the transgene border	Chromosome no. (clone name)
UAS-H1/FGF-7	CAAGAATATTAA(transgene)TTAATAAACTACCA	Chromosome 8 (Bm_scaf51)

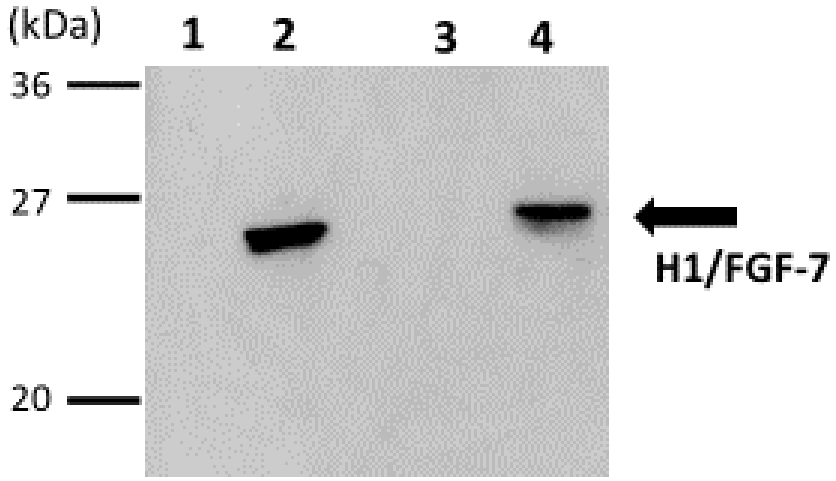

Figure 3-2. Immunoblotting analysis of H1/FGF-7 expressed in posterior silk glands. Protein samples from 50,000 empty polyhedra cubes (negative control; lane 1) and pFGF-7 (positive control; lane 2) produced in baculovirus-infected Sf21 cells, in addition to proteins immunoprecipitated from 50 mg PSGs from *w1-pnd* (lane 3) and FH-H1/FGF-7 larvae (lane 4) were electrophoresed on 12.5% SDS-PAGE and analyzed by immunoblotting with anti-FGF-7 antibodies. Protein size markers are indicated on the left.

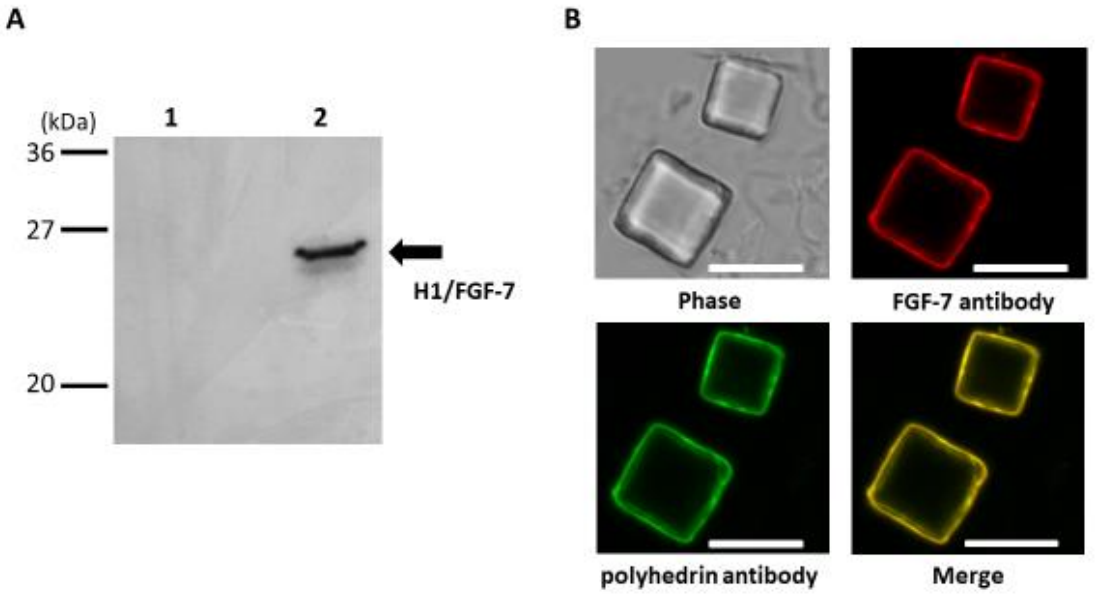

Figure 3-3. Detection of H1/FGF-7 associated with polyhedra. (A) Detection of H1/FGF-7 in polyhedra using immunoblotting. Polyhedra (50,000 cubes) collected from PSGs of FH-polyhedrin (lane 1, ref. 10) and FH-poly/H1/FGF-7 larvae (lane 2) were analyzed using immunoblotting with anti-FGF-7 antibodies. (B) Confocal microscopy analysis of H1/FGF-7 and polyhedrin expression on polyhedra by immunofluorescence. Polyhedra collected from PSGs of FH-poly/H1/FGF-7 larvae were fixed on a glass-base dish and examined using immunofluorescence with anti-FGF-7 antibody and anti-polyhedrin antibody. Scale bars, 10 μm.

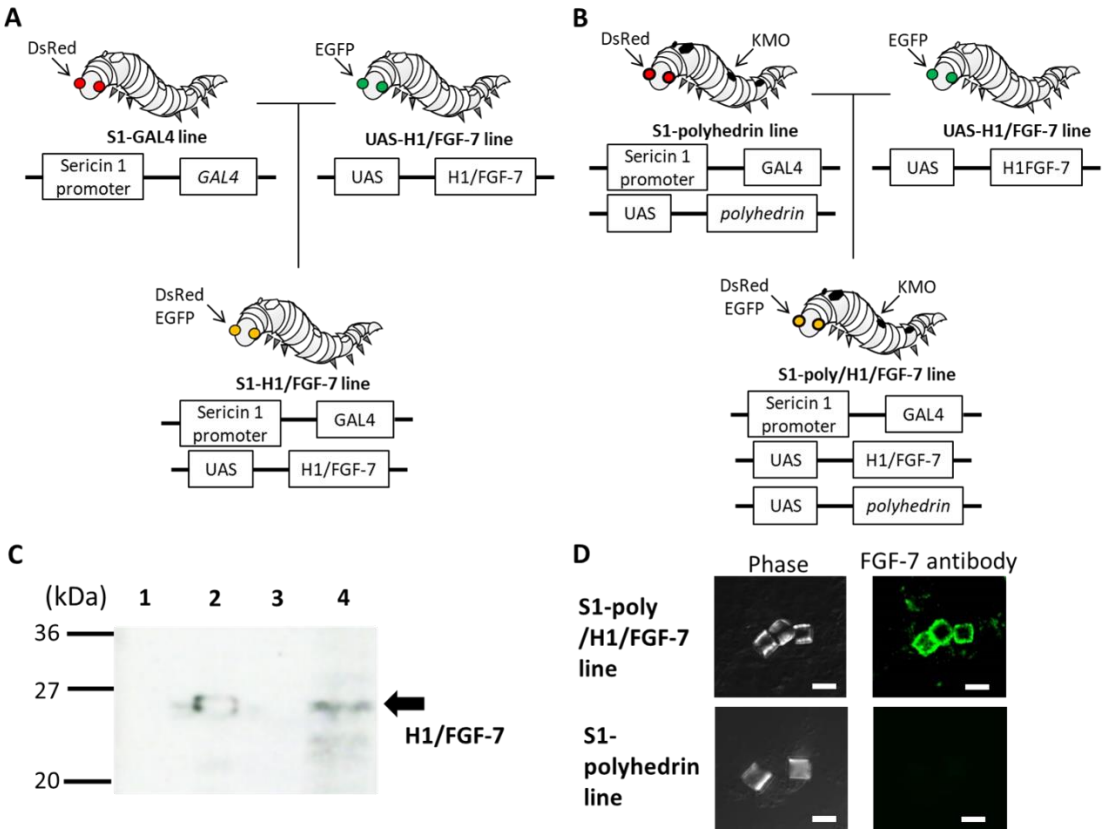

Figure 3-4. Generation of transgenic silkworms expressing H1/FGF-7 in the MSG. (A) Generation of the S1-H1/FGF-7 line. The S1-GAL4 line [60] was mated with the UAS-H1/FGF-7 line to generate the S1-H1/FGF-7 line with EGFP and DsRed expression in the eyes. (B) Generation of the S1-poly/H1/FGF-7 line. The S1-polyhedrin line was mated with the UAS-H1/FGF-7 line to generate the S1-poly/H1/FGF-7 line with EGFP and DsRed expression in the eyes and KMO-specific skin [16]. (C) Immunoblotting analysis of H1/FGF-7 expression in MSGs with 12.5% SDS-PAGE and anti-FGF-7 antibodies. Lane 1 and 2: Protein from 50,000 cubes of empty polyhedra (negative control) and FGF-7-polyhedra (positive control) produced in baculovirus-infected Sf21 cells, respectively; Lanes 3 and 4: Immunoprecipitated protein from 50 mg MSGs from *w1-pnd* and S1-H1/FGF-7 larvae, respectively. Protein size markers are indicated. (D) Confocal immunofluorescence microscopy analysis of H1/FGF-7 on polyhedra. Polyhedra collected from S1-poly/H1/FGF-7 or S1-polyhedrin larvae MSGs were fixed on a glass-based dish and examined by an immunofluorescence with an anti-FGF-7 antibody. Scale bars, 10 μm.

Release of FGF-7 from posterior silk gland powders incorporating pFGF-7

Next, I focused on the ability of pFGF-7 in silk gland material to influence keratinocyte proliferation. I recently reported that upon introduction into cell culture, polyhedra are gradually proteolyzed by cell-derived matrix metalloproteinases (MMPs) and release encapsulated proteins into the culture medium [Publication List 1]. The PSGs from FH-poly/H1/FGF-7 larvae were processed into a fine powder (PSGP; 1.0 mg) and added to the KCM that would contain keratinocyte MMPs to assess the biological properties of pFGF-7 in SGPs. The PSGPs were incubated in culture for 14 days, and media was collected on days 3, 7, 10, and 14 to examine H1/FGF-7 release by ELISA (Figure 3-5). I also measured the released H1/FGF-7 from pFGF-7 (5.0×10^5 cubes) produced in baculovirus-infected Sf21 cells. Five times the amount of polyhedra required for inducing keratinocyte proliferation was used [4]. Until day 14, H1/FGF-7 was continuously detected in media incubated with pFGF-7 (Figure 3-5A) and PSGPs of FH-poly/H1/FGF-7 (Figure 3-5B).

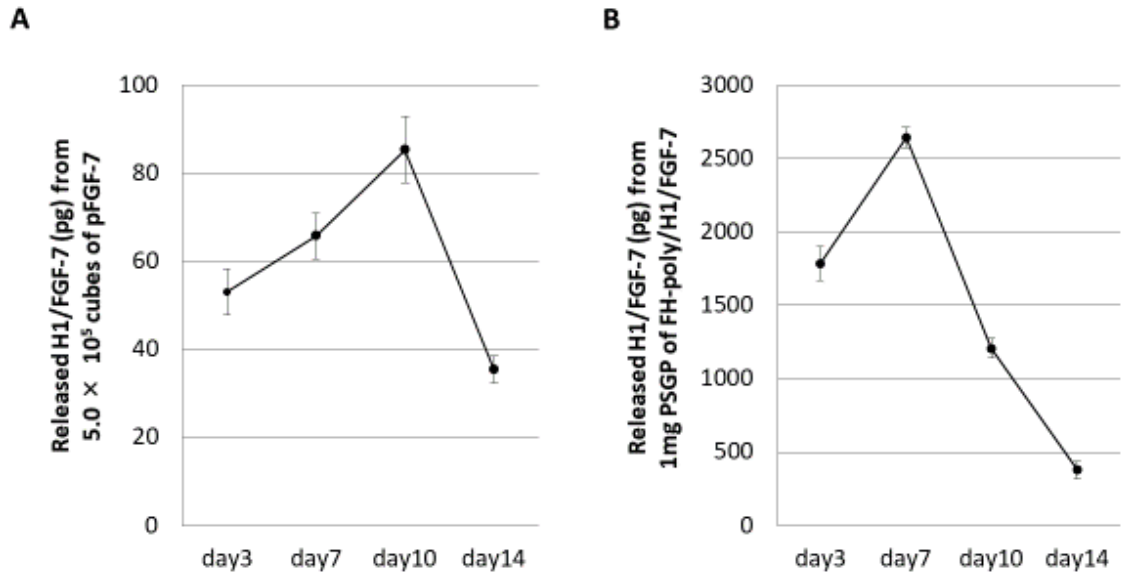

Figure 3-5. Release of H1/FGF-7 from posterior silk gland powders incorporating FGF-7-polyhedra. The amount of H1/FGF-7 released from (A) H1/FGF-7-polyhedra (pFGF-7; 5.0 × 10^5 cubes) or (B) Posterior silk gland powders (PSGP; 1.0 mg) from FH-poly/H1/FGF-7 larvae were examined using an enzyme-linked immunosorbent assay (ELISA) with anti-FGF-7 antibody. Each sample was added into keratinocyte-conditioned media using the filter of a cell culture insert (see MATERIALS AND METHODS) and incubated for 14 days. The medium was changed and collected on days 3, 7, 10, and 14. The amount of FGF-7 in the collected culture medium was determined using an ELISA. Data shown are the means ± standard deviation (SD) of triplicate assays (N = 3 independent samples).

Biological activity of H1/FGF-7 expressed in silk glands

FGF-7 stimulation induces intracellular signaling events such as phosphorylation of receptor-mediated p44/p42 mitogen-activated protein kinase (MAPK) [4]. To assess the biological activity of H1/FGF-7, MSGPs or PSGPs were added to the medium of supplement-starved NHEKs through a cell culture insert filter and incubated for 1 hr before immunoblotting of cell lysates with a phospho-p44/p42 MAPK-specific antibody (Figure 3-5A). Phosphorylation of NHEK p44/p42 MAPK was induced using MSGPs from S1-H1/FGF-7 (lane 4) and S1-poly/H1/FGF-7 (lane 5), and PSGPs from FH-H1/FGF-7 (lane 6) and FH-poly/H1/FGF-7 larvae (lane 7) as well as by rhFGF-7 as a positive control (lane 8). No increase in phosphorylation was observed with no SGPs (lane 1), or with MSGPs from S1-polyhedrin (lane 2) or PSGPs from FH-polyhedrin larvae (lane 3; Figure 3-6A). There was a ~2 mm distance between cells and SGPs in cell culture insert filters. These results indicate that biologically active H1/FGF-7 released from the SGPs could diffuse into the medium and pass through the filter to stimulate p44/p42 MAPK phosphorylation to reach levels that were comparable to those seen for rhFGF-7.

After the culture of supplement-starved NHEKs with SGPs for 72 hr, cell proliferation was determined with a WST-8 assay to detect levels of intracellular

dehydrogenase. The NHEKs were cultured with rhFGF-7 as a positive control, or with no SGPs, MSGPs from S1-polyhedrin or PSGPs from FH-polyhedrin larvae as negative controls. The SGPs from S1-H1/FGF-7, S1-poly/H1/FGF-7, FH-H1/FGF-7, and FH-poly/H1/FGF-7 larvae all dose-dependently induced NHEK proliferation to levels comparable to those seen for the positive control rhFGF-7 (Figure 3-6B). There was a significant increase in the relative number of living cells in cultures treated with 500 μg MSGPs incorporating H1/FGF-7 (S1-H1/FGF-7: ~1.4-fold increase, $P < 0.05$; S1-poly/H1/FGF-7: ~1.3-fold increase, $P < 0.05$) or 200 μg of PSGPs (FH-H1/FGF-7: ~1.9-fold increase, $P < 0.01$; FH-poly/H1/FGF-7: ~2.4-fold increase, $P < 0.01$) over that seen for cells treated with the same amount of SGPs without H1/FGF-7 (Figure 3-5B). However, the relative amount of cell proliferation induced by MSGPs from S1-H1/FGF-7 and S1-poly/H1/FGF-7 larvae was lower than that for PSGPs from FH-H1/FGF-7 and FH-poly/H1/FGF-7 larvae, even though higher amounts of MSGPs were added (50, 250, and 500 μg vs. 50, 100, and 200 μg). The activities inducing the cell proliferation of the PSGPs from FH-H1/FGF-7 and FH-poly/H1/FGF-7 larvae were nearly five-fold higher than that of same amount of MSGPs from S1-H1/FGF-7 and S1-poly/H1/FGF-7 larvae. The PSGPs from FH-poly/H1/FGF-7 larvae also induced more cell proliferation than did FH-H1/FGF-7 (Figure 3-6B). Overall, these results demonstrate that H1/FGF-7 released

from both MSGPs and PSGPs is biologically active and can stimulate keratinocyte proliferation.

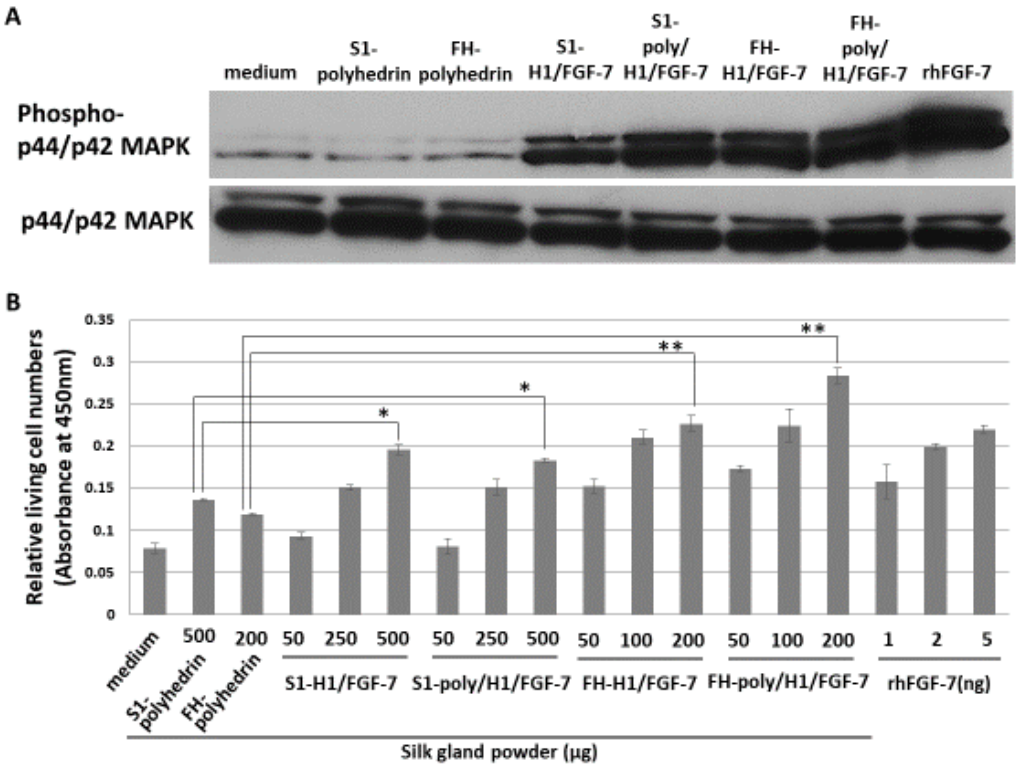

Figure 3-6. Proliferation of NHEK induced by silk gland powders (SGPs) containing pFGF-7. (A) Phosphorylation of p44/42 mitogen-activated protein kinase (MAPK) in cultured NHEKs. NHEKs were supplement-starved overnight and left untreated as a negative control (no SGPs; lane 1) or treated with 10 mg of MSGPs from S1-polyhedrin (lane 2), S1-H1/FGF-7 (lane 4) or S1-poly/H1/FGF-7 larvae (lane 5), or 10 mg of PSGPs from FH-polyhedrin (lane 3), FH-H1/FGF-7 (lane 6) or FH-poly/H1/FGF-7 larvae (lane 7) for 1 hr. NHEKs were also treated with 100 ng/ml rhFGF-7 (lane 8) as a positive control. The NHEK lysates were examined using immunoblotting with antibodies against either p44/p42 MAPK or phosphorylated p44/p42 MAPK. (B) Keratinocyte proliferation. Relative numbers of living cells were determined using a WST-8 assay. NHEKs were cultured in media containing rhFGF-7 (1 ng, 2 ng or 5 ng) or cultured with cell culture inserts with middle silk gland powders from S1-polyhedrin (500 μg), S1-H1/FGF-7 (50 μg, 250 μg or 500 μg) or S1-poly/H1/FGF-7 larvae (50 μg, 250 μg or 500 μg), or posterior silk gland powders from FH-polyhedrin (200 μg), FH-H1/FGF-7 (50 μg, 100 μg or 200 μg) or FH-poly/H1/FGF-7 larvae (50 μg, 100 μg or 200 μg). After incubation for 72 hr, cell numbers were analyzed using a WST-8 assay. Absorbance at 450 nm was determined using a microplate reader. Data are the mean ± SD of triplicate assays. **P* <0.05, ***P* <0.01.

Construction of 3D cultures of keratinocytes with posterior silk gland powders incorporating pFGF-7

Three-dimensional NHEK cultures can be used as a model of human epidermis to substitute for *in vivo* tests involving animals, which successfully assess skin irritations caused by the acute toxicity [26, 27], allergenicity [28], and inflammation [29] of test compounds. I used PSGPs with pFGF-7 to construct a 3D epidermis model to examine the gradual release of H1/FGF-7 from these polyhedra. The NHEKs were cultured on type 1 collagen gels containing PSGPs from FH-polyhedrin or FH-poly/H1/FGF-7 larvae in a basal medium without added rhFGF-7. After replacing the basal medium with a differentiation medium containing Ca^{2+}, air-liquid-interface cultivation was continued for 14 days. The NHEKs were also cultured on gels with basal media and differentiation media with rhFGF-7 and without added PSGPs. The differentiation media was replaced twice weekly. NHEK differentiation was induced at the air-liquid interface, and the enucleation of keratinocytes was verified by HE staining (Figure 3-7A). The 3D cultures with added PSGPs of FH-polyhedrin larvae and rhFGF-7 did not induce sufficient proliferation and adequate differentiation based on negative HE staining and a lack of an enucleated cell layer in the upper parts of the cell culture. However, microscopic observation of the 3D culture of HE-stained NHEK treated with PSGPs from FH-

poly/H1/FGF-7 larvae did reveal sufficient cell proliferation and a well-developed upper layer of enucleated cells corresponding to epidermal morphogenesis (Figure 3-7A).

NHEK 3D cultures with PSGPs from FH-poly/H1/FGF-7 larvae were further examined using immunofluorescence (Figure 3-7B). Cells in the 3D culture were stained with antibodies for keratin 14, which is a stratum basal layer marker, keratin 10, which is a stratum spinosum marker, and loricrin and filaggrin, which are stratum corneum-specific markers. Keratin 10 and keratin 14 staining demonstrated that keratinocyte differentiation and localization were induced during cultivation. Similarly, the loricrin- and filaggrin-positive layer exhibited a well-formed stratum corneum in 3D cultures of NHEK treated with FH-poly/H1/FGF-7 larvae PSGPs (Figure 3-7B), demonstrating that H1/FGF-7 released from PSGPs could induce epidermal morphogenesis with the expected expression of epidermal markers.

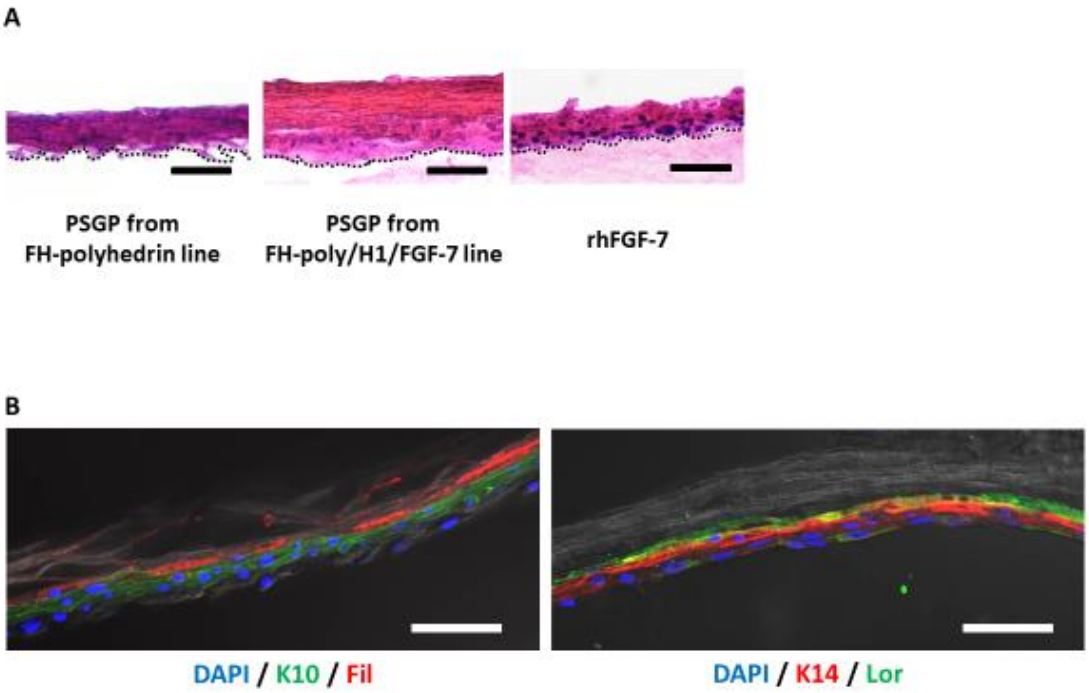

Figure 3-7. 3D keratinocyte cultures. (A) Hematoxylin and eosin (HE) staining in a 3D culture of keratinocytes. NHEKs were cultured on a collagen gel containing 800 μg posterior silk gland powders (PSGPs) from FH-polyhedrin or FH-poly/H1/FGF-7 larvae in the basal medium for two days and in a differentiation medium (basal medium containing 1.2 mM Ca^{2+}) for 14 days. The NHEKs were cultured in the same way on collagen with 100 ng/ml rhFGF-7 in basal and differentiation media as a control. After cultivation for 14 days in differentiation media, 3D cultures were sectioned, subjected to HE staining and observed under a microscope. Scale bar, 50 μm. (B) Immunohistochemical staining of keratinocyte 3D cultures. Immunohistochemical staining of keratin 10 (K10), keratin 14 (K14), Loricrin (Lor), and Filaggrin (Fil) in 3D cultures of keratinocytes incubated with PSGPs from FH-poly/H1/FGF-7 larvae. Nuclei were stained with 4′,6-diamidino-2-phenylindole. Scale bar, 50 μm.

DISCUSSION

In this study, I report that the generation of transgenic silkworms with silk gland cells containing CPV polyhedra that encapsulate H1/FGF-7. H1/FGF-7 and polyhedrin genes were controlled by either the *FH* or *S1* promoter, which are both upregulated upon ecdysteroid secretion, which occurs during the late stage of the 5th instar. The amount of pFGF-7 in the silk glands is predicted to be maximized during the spinning stage after a gut purge, as was previously observed for the production of FGF-2 [16]. Thus, biologically active H1/FGF-7 would be present in polyhedra in SGP during the spinning stage of larval development.

Immunofluorescence detected with an FGF-7 antibody showed specific H1/FGF-7 signals near the polyhedra surface (Figure 3-3B). FGF-7 has a very short half-life of biological activity due to low protein stability [3, 55]. However, the assays of NHEK proliferation that were performed for this study demonstrated that long-term, stable H1/FGF-7 activity was maintained in PSGPs (Figure 3-6). Moreover, SGPs with pFGF-7 induced a higher amount of NHEK proliferation than SGPs containing only H1/FGF-7 without polyhedra (Figure 3-6), demonstrating that encapsulation of H1/FGF-7 in polyhedra in transgenic PSGs could maintain stable bioactivity of H1/FGF-7 in the silkworm body or SGPs. It is still unclear whether the addition of an H1-tag to the N-

terminus of FGF-7 affects its ability to induce keratinocyte proliferation. However, I did not find a remarkable loss in the bioactivity of H1/FGF-7 through the addition of H1-tag in this and a previous study [4].

Research has shown that degummed fibroin can preserve cell growth factor activity even after processing solubilized fibroin into re-crystalized sponges or films [20, 21]. In addition, crystalized fibroin, which forms a layer of fibroin in silkworm cocoons, can protect the bioactivity of recombinant proteins expressed in PSGs, or those secreted into the PSG lumen and subsequently embedded in fibroin crystals during spinning [17-19]. In this study, H1/FGF-7 was not secreted into the fibroin layer of the cocoon. Instead, it was likely embedded in fibroin crystals formed during freeze-drying [61]. H1/FGF-7 activity was stably maintained during physical processing of the fibroin such that PSGs with free H1/FGF-7 could still induce NHEK proliferation (Figure 3-6). From this perspective, the activity of cytokines contained in PSGs withstands physical processing. Weak activities were shown in the media with MSGPs from S1-polyhedrin or PSGPs from FH-polyhedrin larvae after the 3 day incubation, as with the previous reports that fibroin [62] and sericin [63] of silkworm SGPs have slight activities to stimulate mammalian cell proliferation.

I also found that MSGPs incorporating pFGF-7 induced NHEK proliferation,

although to a lesser extent than that observed for PSGPs. One possible explanation for this weaker activity is that silk proteins in liquid form in PSGs are carried into and accumulate in MSGs such that the relative concentration of H1/FGF-7 in MSGPs would be lower than that in PSGPs. However, MSGs can be processed into fibrous materials, such as silk guts, because of the high amount of liquid fibroin they contain. For effective use of MSG fibrous materials to control cell proliferation, systems to express foreign proteins in MSGs could be improved through various modifications, such as enhanced promoter activity, which is achieved by the introduction of a baculovirus *hr3* sequence in the region upstream of the promoter [17, 19].

I also showed that PSGPs with pFGF-7 continued to release H1/FGF-7 for at least 14 days, as with pFGF-7 (Figure 3-5). Posterior silk gland materials that incorporate polyhedra that encapsulate cytokines could thus serve as effective cytokine carriers for tissue engineering applications and could be used as a platform to continuously release diverse cytokines. In addition, PSGPs incorporating pFGF-7 can be used in the construction of a human epidermis model that requires sustainable supplies of cell growth factors to achieve long-term cultivation (Figure 3-7). Typically, epidermal cultures require fresh media that are supplemented with fresh cytokines every 2–3 days [64-66]. NHEK 3D cultures that maintain an air-liquid interface over the long-term are challenging

to manipulate, and the replacement of medium can inhibit the appropriate formation of the epidermis. Here I revealed that the introduction of pFGF-7-incorporating PSGPs effectively induced keratinocyte proliferation and differentiation into a stratified epidermis that expressed the expected epidermal differentiation protein markers (Figure 3-6A and Figure 3-6B). As described, the medium of the 3D culture was changed every 3–4 days (twice weekly), but stratified epidermis did not form with the addition of only rhFGF-7 (Figure 3-7A), suggesting the need for more frequent replacement of medium supplemented with rhFGF-7 than was previously recommended [64-66]. I showed that, even with infrequent medium replacement, PSGP-containing polyhedra that incorporate H1/FGF-7 induced keratinocyte proliferation and differentiation into the stratified epidermis. Thus, polyhedra incorporating H1/FGF-7 could be a useful tool for generating and maintaining 3D NHEK cultures for use as *in vitro* epidermal models.

Here I used pFGF-7-incorporating PSGPs to control the proliferation and differentiation of NHEKs, although methods involving lysis, crushing, and sonication of SGPs have recently been developed to prepare polyhedra from MSGPs of transgenic silkworms [Publication List 3]. Using these steps to remove the PSG component enables the use of prepared polyhedra from individual silkworms as an effective protein production host for tissue engineering. Cytokine-encapsulated polyhedra have typically

been isolated from recombinant baculovirus-infected insect cultured cells, although such culture systems do raise concerns about the presence of amphixenotic pathogens that could contaminate animal serum added to cell culture media. In addition, baculovirus shows some immunostimulatory activity toward mammalian cells [15]. The foreign protein expression system I used in transgenic silkworms does not involve viral vectors or animal serum for *in vitro* cell culture. Therefore, it is useful for generating artificial materials that mimic the extracellular matrices or cell scaffolds that locally release cell growth factors. Such materials would be valuable for grafts and other applications. The sericulture industry has effective systems for the large-scale production of SGPs that can be used to produce not only *in vitro* cell culture models but also artificial materials for clinical use [54].

In conclusion, I describe the genetic engineering of a silkworm line for the production of posterior silk gland materials that incorporate FGF-7 protein microcrystals that protect and release FGF-7 activity. These silk gland materials have the potential to control keratinocyte proliferation and differentiation for the generation of human epidermis models for *in vitro* applications. The results of this study will be useful for the development of silk gland materials for cell engineering purposes, both *in vivo* and *in vitro*.

Chapter 4

General Discussion

In Chapter 2, I reported two essential results: (1) the alignment of differentiated PC12 cells at the periphery of pNGF spots and (2) the release of NGF from pNGF mediated by MMPs secreted from PC12 cells. In Chapter 3, I detailed the generation of transgenic silkworm that expressed pFGF-7 in their PSG and MSG. This recombinant protein expression system in silk glands enabled us to obtain polyhedra-encapsulated cell growth factors under virus-free and serum-free conditions. The activated pFGF-7 in MSGPs and PSGPs induced keratinocyte proliferation. The PSGPs released H1FGF-7 continuously for at least 14 days in the MMP-rich [67] keratinocyte conditioned medium. I successfully constructed a 3D epidermal model with pFGF-7 expressed in PSGPs *in vitro*. In the 3D epidermal model, I observed sufficient cell proliferation and a well-developed upper layer of differentiation marker-positive enucleated cells.

I determined that the alignment of differentiated PC12 cells in pNGF would be a useful tool for the repair or regeneration of nerve fibers. However, the alignment is currently short, and an *in vivo* application has yet to be developed. A new cell culture system with a combination of silk and polyhedra should be developed to solve these problems. Silk has previously been used as a biomaterial to promote axonal regeneration [13, 68, 69]. The cortical nerve cell spheres adhere to the silk fibroin fibers and stretch the neurites on the fibers to connect with each other. The axons can cover long distances,

e.g. several millimeters in length, by connecting the consecutively adjacent spheres [68]. Furthermore, the silk fibroin scaffold containing NGF is biocompatible with PC12 cells and supports the neuronal differentiation of these cells even when NGF is absent from the media [13, 69]. PSGs can be processed into fibrous materials such as silk guts. The earlier study [16] showed that silk guts processed from PSGs expressing H1/FGF-2-encapsulating polyhedra (pFGF-2) induced the proliferation of NIH3T3 cells. Moreover, the powder processed from silk guts containing pFGF2 retained FGF-2 activity for one week at 25°C. Therefore, I considered that silk guts processed from PSGs expressing polyhedra-encapsulated neurotrophic factors, such as NGF, would be suitable scaffolds for promoting long axonal regeneration i*n vivo*.

Target protein-encapsulating polyhedra systems have also been used for the development of vaccines. For example, I previously attempted to generate norovirus-like particle-encapsulating polyhedra (pNoVLP) for an oral vaccine [70]. Noroviruses are important pathogens that affect millions of people worldwide by causing acute epidemic gastroenteritis. It is impossible to multiply norovirus by artificial means, so virus-like particles are used to develop the vaccine instead [71]. To use pNoVLP as oral vaccine, pNoVLP should be produced in virus-free and serum-free; however, it has been produced in a baculovirus-infected Sf21 cell line. I addressed this problem in Chapter 3, in which I

showed that FGF-7 could be encapsulated into polyhedra in silk glands expressing FGF-7 and polyhedrin, similar to pFGF-7 produced in Sf21 cell lines. A previous study has shown the ease of purifying polyhedra from silk glands [Publication List 3]. To produce polyhedra without using serums and viruses and enabling their application *in vivo*, transgenic silkworm can be used to produce target protein-encapsulating polyhedra.

The size of polyhedra produced in baculovirus-infected Sf21 cells is around 5 μm [4-11]; however, the polyhedra produced in silk gland cells are larger at around 10 μm. Polyhedra are collected by centrifugation after denaturation of the cells expressing them. Polyhedra that are too small cannot be collected because they do not precipitate; hence, the polyhedra collection rate would likely increase if they are larger, as is the case with silkworm polyhedra. In transgenic silkworm, ecdysteroid secretion upregulates target gene expression during the late stage of the fifth instar [16]. Some polyhedra are formed in PSGs from the late stage of the fourth instar to the first stage of the fifth instar. The size and number of polyhedra then increase substantially on the sixth day of the fifth instar [16]. The polyhedra produced in PSG cells form within a few days at the late stage of the fifth instar. In contrast, it takes 10 days to collect polyhedra after transferring baculoviruses into Sf21 cells. These results demonstrate that the protein expression system in transgenic silkworm is efficient for polyhedra expression. Nevertheless, the

production of polyhedra in transgenic silkworm does have disadvantages. For example, microinjection equipment and techniques are necessary to generate transgenic silkworm; acquiring the necessary skill to administer these microinjections takes a considerable amount of time. On the other hand, producing polyhedra in baculovirus-infected Sf21 cells is easier because the baculovirus needs only to be transferred into the Sf21 cells and incubated for 10 days.

I successfully constructed an epidermal model by using PSGP-containing pFGF-7. I found that NHEK stratified more than the model incubated with rhFGF-7. Immunostaining showed that the model incubated with PSGP-containing pFGF-7 expressed keratinocyte differentiation markers at each layer of the epidermis (Figure 3-7). However, the layer expressing loricrin was very close to the expression layer of keratin 14. Loricrin expresses at the layer of the stratum corneum and stratum granulosum. This result suggests that the model would be induced more differentiation compared with the epidermis *in vivo*. FGF-7 is an important growth factor in the construction of the epidermal model for inducing keratinocyte proliferation and adjusting the morphology of differentiated keratinocytes in the epidermis [25]. The PSGP-containing pFGF-7 in collagen gel might have released less FGF-7 than that of pFGF-7 incubated in a conditioned medium in an ELISA (Figure 3-5), which showed continuous FGF-7 release

for 14 days. This is likely because the keratinocytes were not in contact with the medium during the 14-day air-liquid interface cultivation. To induce additional FGF-7 release from PSGPs with pFGF-7 in the collagen gel, MMP-rich conditioned medium could be used. Releasing more FGF-7 would increase the life span of keratinocytes and improve the tissue architecture of the epidermal model.

Here, we reported the generation of transgenic silkworm expressing pFGF-7 in their silk glands as well as the effects of the silk materials processed from the silk glands *in vitro*. Besides, I attempted to generate transgenic silkworms that produce cocoons containing FGF-2, FGF-7, and polyhedrin. Silkworm cocoons are mainly composed of sericin and fibroin expressed in MSGs and PSGs, respectively. Target proteins are expressed in MSGs or PSGs and then secreted into sericin or fibroin layers in silk cocoons by using signal peptide for secretion with sericin or as a fusion protein with fibroin, respectively [17, 18]. The natural ratio of fibroin to sericin is approximately 3:1. PSGs might produce more recombinant protein than MSGs; however, PSGs have disadvantages because they secrete target proteins in the insoluble fibroin layer. Thus, strong denaturing agents are required to extract expressed proteins embedded in the fibroin layer, and the proteins' bioactivities are largely lost during the extraction process [17, 18]. In contrast, the proteins secreted in the sericin layer can be extracted easily by placing the cocoon in

a mild solution, such as PBS or water, because sericin is much more hydrophilic than fibroin [17, 18]. Furthermore, the lower expression efficiency of the MSG compared to the PSG can be solved by introducing an enhancer such as the baculovirus *hr3* sequence in the region upstream of the *sericin* promoter [19].

In the research, I attempted to generate transgenic silkworms that produce sericin cocoons containing polyhedrin and FGF-7 (Maruta, personal communication). These silkworms secreting FGF-7 and polyhedrin into the sericin layer of their cocoon were mated with silkworms spinning only sericin cocoons due to specific dysfunction of PSGs expressing the cabbage butterfly (*Pieris rapae)* cytotoxin pierisin-1A (P1A) [53]. The introduction of P1A caused the failure of PSGs to produce fibroin; thus, this silkworm made a cocoon consisting solely of sericin [53]. Sericin has many characteristics that are relevant to biomedical applications, including biocompatibility, mechanical stability, biodegradability, and anti-bacterial activity [Publication List 4, 72]. I collected sericin cocoons containing FGF-7 and polyhedrin and applied these in cell cultures. In the sericin cocoons, polyhedrin did not crystallize into polyhedra (Maruta, personal communication). However, the sericin cocoons released FGF-7 continuously for 21 days and induced cell proliferation and migration. The amount of FGF-7 in the sericin cocoons was much higher than that of FGF-7 in PSGPs. This evidence suggests that FGF-7-containing sericin

cocoons would be suitable materials for wound healing, in which high concentrations of FGF-7 are required. In contrast, PSGs expressing pFGF-7 would be useful for producing polyhedra in virus-free and serum-free systems as well as silk guts containing pFGF-7.

In Chapters 2 and 3, I described the use of growth factors encapsulated in polyhedra produced in baculovirus-infected Sf21 cells and the silk glands of transgenic silkworms, respectively. In both cases, the polyhedra produced slowly released the encapsulated active growth factors and maintained their biological activities over long periods. In clinical settings, current growth factor medications are often unsafe and costly because they require high doses and/or repeated administrations due to the short half-life of the growth factors *in vivo*. Polyhedra technologies could overcome these problems because they represent ideal DDS materials that can release encapsulated active growth factors over long periods. PSGP-containing polyhedra might have better effects than polyhedra for this purpose because silk fibroin has cell growth activity in some cells. Nevertheless, further research into *in vivo* approaches by which substances, including cytokine-encapsulating polyhedra and silk proteins, can be used to control cell proliferation or differentiation will be necessary to develop effective biomaterials for tissue engineering.

REFERNCES

1. Yamakawa, S. and Hayashida, K. (2019) Advances in surgical applications of growth factors for wound healing. *Burns Trauma* **7**, 10
2. Koria, P. (2012) Delivery of Growth Factors for Tissue Regeneration and Wound Healing. BioDrugs 26, 163–175
3. Rohrmann, G. F. (1986) Polyhedrin structure. *J. Gen. Virol.* **67**, 1499–1513
4. Ijiri, H., Coulibaly, F., Nishimura, G., Nakai, D., Chiu, E., Takenaka, C., Ikeda, K., Nakazawa, H., Hamada, N., Kotani, E., Metcalf, P., Kawamata, S., and Mori, H. (2009) Structure-based targeting of bioactive proteins into cypovirus polyhedra and application to immobilized cytokines for mammalian cell culture. *Biomaterials* **30**, 4297–4308
5. Ikeda, K., Nagaoka, S., Winkler, S., Kotani, K., Yagi, H., Nakanishi, K., Miyajima, S., Kobayashi, J., and Mori, H. (2001) Molecular characterization of *Bombyx mori* cytoplasmic polyhedrosis virus genome segment 4. *J. Gen. Virol*. **75**, 988–995
6. Ikeda, K., Nakazawa, H., Shimo-Oka, A., Ishio, K., Miyata, S., Hosokawa, Y., Matsumura, S., Masuhara, H., Belloncik, S., Alain, R., Goshima, N., Nomura, N., Morigaki, K., Kawai, A., Kuroita, T., Kawakami, B., Endo, Y., and Mori, H. (2006) Immobilization of diverse foreign proteins in viral polyhedra and potential application

for protein microarrays. *Proteomics* **6**, 54–66

7. Yuasa, H., Kotani, E., Mori, H., and Takaki, K. (2020) New method for immobilising diverse proteins onto cubic micro-protein polyhedrin crystals. *Protein Expr. Purif.* **167**, 105531
8. Matsumoto, G., Hirohata, R., Hayashi, K., Sugimoto, Y., Kotani, E., Shimabukuro, J., Hirano, T., Nakajima, Y., Kawamata, S., and Mori, H. (2014) Control of angiogenesis by VEGF and endostatin-encapsulated protein microcrystals and inhibition of tumor angiogenesis. *Biomaterials* **35**, 1326–1333
9. Mori, H., Shukunami, C., Furuyama, A., Notsu, H., Nishizaki, Y., and Hiraki, Y. (2007) Immobilization of bioactive fibroblast growth factor-2 into cubic proteinous microcrystals (*Bombyx mori* Cypovirus polyhedra) that are insoluble in a physiological cellular environment. *J. Biol. Chem.* **282**, 17289–17296
10. Nishishita, N., Ijiri, H., Takenaka, C., Kobayashi, K., Goto, K., Kotani, E., Itoh, T., Mori, H., and Kawamata, S. (2011) The use of leukemia inhibitory factor immobilized on virus-derived polyhedra to support the proliferation of mouse embryonic and induced pluripotent stem cells. *Biomaterials* **32**, 3555–3563
11. Ijiri, H., Nakatani, T., Ido, H., Hamada, N., Kotani, E., and Mori, H. (2010) Immobilization of protein kinase C into Cypovirus polyhedra. *J. Insect*

Biotechnol. Sericol. **79**, 1015–1020

12. Matsumoto, G., Ueda, T., Shimoyama, J., Ijiri, H., Omi, Y., Yube, H., Sugita, Y., Kubo, K., Maeda, H., Kinoshita, Y., Arias, D.G., Shimabukuro, J., Kotani, E., Kawamata, S., Mori, H. (2012) Bone regeneration by polyhedral microcrystals from silkworm virus. *Sci Rep*. **2**, 935.
13. Tian, L., Prabhakaran, M. P., Hu, J., Chen, M., Besenbacher, F., and Ramakrishna, S. (2015) Coaxial electrospun poly (lactic acid)/silk fibroin nanofibers incorporated with nerve growth factor support the differentiation of neuronal stem cells. *RSC Adv.* **5**, 49838–49848
14. Patel, S., Kurpinski, K., Quigley, R., Gao, H., Hsiao, B. S., Poo, M.-M., and Li, S. (2007) Bioactive Nanofibers: Synergistic Effects of Nanotopography and Chemical Signaling on Cell Guidance. *Nano Lett.* **7**, 2122–2128
15. Kataoka, C., Kaname, Y., Taguwa, S., Abe, T., Fukuhara, T., Tani, H., Moriishi, K., and Matsuura, Y. (2012) Baculovirus GP64-mediated entry into mammalian cells. *J. Virol*. **86**, 2610–2620
16. Kotani, E., Yamamoto, N., Kobayashi, I., Uchino, K., Muto, S., Ijiri, H., Shimabukuro, J., Tamura, T., Sezutsu, H., and Mori, H. (2015) Cell proliferation by silk gut incorporating FGF-2 protein microcrystals. *Sci. Rep*. **5**, 11051

17. Tomita, M., Hino, R., Ogawa, S., Iizuka, M., Adachi, T., Shimizu, K., Hisaya, S., and Yoshizato, K. (2007) A germline transgenic silkworm that secretes recombinant proteins in the sericin layer of cocoon. *Transgenic Res.* **16**, 449–465

18. Tatematsu, K., Kobayashi, I., Uchino, K., Sezutsu, H., Iizuka, T., Yonemura, N., and Tamura, T. (2010) Construction of a binary transgenic gene expression system for recombinant protein production in the middle silk gland of the silkworm *Bombyx Mori*. *Transgenic Res.* **19**, 473–487

19. Wang, F., Xu, H., Yuan, L., Ma, S., Wang, Y., Duan, X., Duan, J., Xiang, Z., and Xia, Q. (2013) An optimized sericin-1 expression system for mass-producing recombinant proteins in the middle silk glands of transgenic silkworms. *Transgenic Res*. **22**, 925–938

20. Kambe, Y., Kojima, K., Tamada, Y., Tomita, N., and Kameda, T. (2016) Silk fibroin sponges with cell growth-promoting Aactivity induced by genetically fused basic fibroblast growth factor. *J. Biomed. Mater. Res. A*. **104**, 82–93

21. Baba, A., Matsushita, S., Kitayama, K., Asakura, T., Sezutsu, H., Tanimoto, A., and Kanekura, T. (2019) Silk fibroin produced by transgenic silkworms overexpressing the Arg-Gly-Asp motif accelerates cutaneous wound healing in mice. *J. Biomed. Mater. Res. B Appl. Biomater.* **107**, 97–103

22. Yagi, T., Sato, M., Nakazawa, Y., Tanaka, K., Sata, M., Itoh, K., Takagi, Y., and Asakura, T. (2011) Preparation of double-raschel knitted silk vascular grafts and evaluation of short-term function in a rat abdominal aorta. *J. Artif. Organs* **14**, 89–99

23. Kuboyama, N., Kiba, H., Arai, K., Uchida, R., Tanimoto, Y., Bhawal, U. K., Abiko, Y., Miyamoto, S., Knight, D., Asakura, T., and Nishiyama, N. (2013) Silk fibroin-based scaffolds for bone regeneration. *J. Biomed. Mater. Res. B Appl. Biomater.* **101**, 295–302

24. Sugihara, A., Sugiura, K., Morita, H., Ninagawa, T., Tubouchi, K., Tobe, R., Izumiya, M., Horio, T., Abraham, N. G., and Ikehara, S. (2000) Promotive effects of a silk film on epidermal recovery from full-thickness skin wounds. *Proc. Soc. Exp. Biol. Med*. **225**, 58–64

25. Seo, A., Kitagawa, N., Matsuura, T., Sato, H., and Inai, T. (2016) Formation of keratinocyte multilayers on filters under airlifted or submerged culture conditions in medium containing calcium, ascorbic acid, and keratinocyte growth factor. *Histochem. Cell Biol.* **146**, 585–597

26. Pedrosa, T. do N., Catarino, C. M., Pennacchi, P. C., Assis, S. R. de, Gimenes, F., Consolaro, M. E. L., Barros, S. B. de M., and Maria-Engler, S. S. (2017) A new

reconstructed human epidermis for *in vitro* skin irritation testing. *Toxicol. Vitro* **42**, 31–37

27. Chen, L., Wu, M., Jiang, S., Zhang, Y., Li, R., Lu, Y., Liu, L., Wu, G., Liu, Y., Xie, L., and Xu, L. (2019) Skin toxicity assessment of silver nanoparticles in a 3D epidermal model compared to 2D keratinocytes. *Int. J. Nanomed.* **14**, 9707–9719
28. Neves, C. R., and Gibbs, S. (2018) Progress on reconstructed human skin models for allergy research and identifying contact sensitizers. *Curr. Top. Microbiol. Immunol.* Springer, Berlin, Heidelberg. 1–27
29. Chung, E., Choi, H., Lim, J. E., and Son, Y. (2014) Development of skin inflammation test model by co-culture of reconstituted 3D skin and RAW264.7 cells. *J. Tissue Eng. Regen. Med.* **11**, 87–92
30. Peng, W.J., Yan, J.W., Wan, Y.N., Wang, B.X., Tao, J.H., Yang, G.J., Pan, H.F., and Wang, J. (2012) Matrix metalloproteinases: A review of their structure and role in systemic sclerosis. *J. Clin. Immunol.* **32**, 1409–1414.
31. Surgucheva, I., Chidambaram, K., Willoughby, D.A., and Surguchov, A. (2010) Matrix metalloproteinase 9 expression: New regulatory elements. *J. Ocul. Biol. Dis. Infor.* **3**, 41–52.

32. Barthes, J., Ozcelik, H., Hindie, M., Ndreu-Halili, A., Hasan, A., and Vrana, N.E. (2014) Cell microenvironment engineering and monitoring for tissue engineering and regenerative medicine: the recent advances. *Biomed Res Int*. **2014**, 921905.

33. Bourget, J.M., Guillemette, M., Veres, T., Auger, F.A., and Germain, L. (2013) Alignment of Cells and Extracellular Matrix Within Tissue- Engineered Substitutes. *In Advances in Biomaterials Science and Biomedical Applications*.

34. Gattazzo, F., Urciuolo, A., and Bonaldo, P. (2014) Extracellular matrix: a dynamic microenvironment for stem cell niche. *Biochim Biophys Acta*. **1840**, 2506-2519.

35. Muiznieks, L.D., and Keeley, F.W. (2013) Molecular assembly and mechanical properties of the extracellular matrix: A fibrous protein perspective. *Biochim Biophys Acta*. **1832**, 866-875.

36. Surguchev, A.A., Emamzadeh, F.N., and Surguchov, A. (2019) Cell responses to extracellular α-synuclein. *Molecules* **24**, 2, 305.

37. Loffek, S., Schilling, O., Franzke, and C.W. Series. (2011) Matrix metalloproteinases in lung health and disease": Biological role of matrix metalloproteinases: a critical balance. *Eur Respir J*. **38**, 1, 191-208.

38. Bhattacharjee, N., and Folch, A. (2017) Large-scale microfluidic gradient arrays reveal axon guidance behaviors in hippocampal neurons. *Microsystems & Nanoengineering* **3**, 17003.

39. Georgiou, M., Golding, J.P., Loughlin, A.J., Kingham, P.J., and Phillips, J.B. (2015) Engineered neural tissue with aligned, differentiated adipose-derived stem cells promotes peripheral nerve regeneration across a critical sized defect in rat sciatic nerve. *Biomaterials* **37**, 242-251.

40. Gnavi, S., Fornasari, B.E., Tonda-Turo, C., Laurano, R., Zanetti, M., Ciardelli, and G., Geuna, S. (2015) The Effect of Electrospun Gelatin Fibers Alignment on Schwann Cell and Axon Behavior and Organization in the Perspective of Artificial Nerve Design. *Int J Mol Sci*. **16**, 12925-12942.

41. Han, D., and Cheung, K.C. (2011) Biodegradable Cell-Seeded Nanofiber Scaffolds for Neural Repair. *Polymers* **3**, 1684-1733.

42. Wang, W., Itoh, S., Konno, K., Kikkawa, T., Ichinose, S., Sakai, K., Ohkuma, T., and Watabe, K. (2009) Effects of Schwann cell alignment along the oriented electrospun chitosan nanofibers on nerve regeneration. *J Biomed Mater Res*. **91**, 994-1005.

43. Skaper, S.D. The neurotrophin family of neurotrophic factors: an overview. (2012) *Methods Mol Biol*. **846**, 1-12.

44. Sofroniew, M.V., Howe, C.L., and Mobley, W.C. (2001) Nerve growth factor signaling, neuroprotection, and neural repair. *Annu Rev Neurosci*. **24**, 1217-1281.

45. Mingorance-Le Meur, A., Mohebiany, A.N., and O'Connor, T.P. (2009) Varicones and growth cones: two neurite terminals in PC12 cells. *PLOS ONE* **4**, e4334.

46. Mori, H., and Metcalf, P. (2010) Cypoviruses. *In Insect Virology*. 307-324.

47. Wang, H., Parry, S., Macones, G., Sammel, M.D., Ferrand, P.E., Kuivaniemi, H., Tromp, G., Halder, I., Shriver, M.D., Romero, R., and Strauss, J.F. (2004) 3rd Functionally significant SNP MMP8 promoter haplotypes and preterm premature rupture of membranes (PPROM). *Hum Mol Genet*, **13**, 2659-2669.

48. Saarialho-Kere, U.K., Crouch, E.C., and Parks, W.C. (1995) Matrix metalloproteinase matrilysin is constitutively expressed in adult human exocrine epithelium. *J Invest Dermatol*. **105**, 190-196.

49. Pollock, J.D., Krempin, M., and Rudy, B. (1990) Differential effects of NGF, FGF, EGF, cAMP, and dexamethasone on neurite outgrowth and sodium channel expression in PC12 cells. *J Neurosci*. **10**, 2626-2637.

50. Drubin, D.G., Feinstein, S.C., Shooter, E.M., and Kirschner, M.W. (1985) Nerve growth factor-induced neurite outgrowth in PC12 cells involves the coordinate

induction of microtubule assembly and assembly-promoting factors. *J Cell Biol*. **101**, 1799-1807.

51. Matsushima, K., Suyama, T., Takenaka, C., Nishishita, N., Ikeda, K., Ikada, Y., Sawa, Y., Jakt, L.M., Mori, H., and Kawamata, S. (2010) Secreted frizzled related protein 4 reduces fibrosis scar size and ameliorates cardiac function after ischemic injury. *Tissue Eng Part A*. **16**, 3329-3341.
52. Shimizu, T., Ishikawa, T., Iwai, S., Ueki, A., Sugihara, E., Onishi, N., Kuninaka, S., Miyamoto, T., Toyama, Y., Ijiri, H., Mori, H., Matsuzaki, Y., Yaguchi, T., Nishio, H., Kawakami, Y., Ikeda, Y., and Saya, H. (2012) Fibroblast growth factor-2 is an important factor that maintains cellular immaturity and contributes to aggressiveness of osteosarcoma. *Mol Cancer Res*. **10**, 454-468.
53. Otsuki, R., Yamamoto, M., Matsumoto, E., Iwamoto, S., Sezutsu, H., Suzui, M., Takaki, K., Wakabayashi, K., Mori, H., and Kotani, E. (2017) Bioengineered silkworms with butterfly cytotoxin-modified silk glands produce sericin cocoons with a utility for a new biomaterial. *Proc. Natl. Acad. Sci. USA* **114**, 6740–6745
54. Kundu, B., Rajkhowa, R., Kundu, S. C., and Wang, X. (2013) Silk fibroin biomaterials for tissue regenerations. *Adv. Drug Deliv. Rev*. **65**, 457–470

55. Huang, Z., Zhu, G., Sun, C., Zhang, J., Zhang, Y., Zhang, Y., Ye, C., Wang, X., Ilghari, D., and Li, X. (2012) A novel solid-phase site-specific pegylation enhances the *in vitro* and *in vivo* biostability of recombinant human keratinocyte growth factor. *PLOS ONE* **7**, e36423

56. Kobayashi, I., Uchino, K., Sezutsu, H., Iizuka, T., and Tamura, T. (2007) Development of a new *piggyBac* vector for generating transgenic silkworms using the kynurenine 3-mono oxygenase gene. *J. Insect Biotechnol. Sericol*. **76**, 145–148

57. Sakudoh, T., Sezutsu, H., Nakashima, T., Kobayashi, I., Fujimoto, H., Uchino, K., Banno, Y., Iwano, H., Maekawa, H., Tamura, T., Kataoka, H., and Tsuchida, K. (2007) Carotenoid silk coloration is controlled by a carotenoid-binding protein, a product of the *Yellow blood* gene. *Proc. Natl. Acad. Sci. USA* **104**, 8941–8946

58. Tamura, T., Thibert, C., Royer, C., Kanda, T., Abraham, E., Kamba, M., Kômoto, N., Thomas, J. L., Mauchamp, B., Chavancy, G., Shirk, P., Fraser, M., Prudhomme, J. C., and Couble, P. (2000) Germline transformation of the silkworm *Bombyx mori* L. using a *piggyBac* transposon-derived vector. *Nat. Biotechnol.* **18**, 81–84

59. Imamura, M., Nakai, J., Inoue, S., Quan, G., Kanda, T., and Tamura, T. (2003) Targeted gene expression using the *GAL4/UAS* system in the silkworm *Bombyx mori*. *Genetics* **165**, 1329–1340

60. Sezutsu, H., Uchino, K., Tatematsu, K., Iizuka, K.-I., Yonemura, T., N., and Tamura, T. (2009) Conservation of fibroin gene promoter function between the domesticated silkworm *Bombyx mori* and the wild silkmoth *Antheraea yamamai*. *J. Insect Biotechnol. Sericol.* **78**, 1–10

61. Magoshi, J. and Nakmura, S. (1987) Structure and thermal properties of silk (in Japanese). *Netsu Sokutei* **14**, 8941–8946

62. Tsubouchi, K., Nakao, H., Igarashi, Y., Takasu, Y., and Yamada, H. (2003) Bombyx mori Fibroin Enhanced the Proliferation of Cultured Human Skin Fibroblasts. *Journal of Insect Biotechnology and Sericology* **72**, 65–69

63. Liu, L., Wang, J., Duan, S., Chen, L., Xiang, H., Dong, Y., and Wang, W. (2016) Systematic evaluation of sericin protein as a substitute for fetal bovine serum in cell culture. *Sci Rep* **6**, 31516

64. Shimabukuro, J., Yamaoka, A., Murata, K.-I., Kotani, E., Hirano, T., Nakajima, Y., Matsumoto, G., and Mori, H. (2014) 3D co-cultures of keratinocytes and melanocytes and cytoprotective effects on keratinocytes against reactive oxygen species by insect virus-derived protein microcrystals. *Mater. Sci. Eng. C Mater. Biol. Appl.* **42**, 64–69

65. Rendl, M., Ban, J., Mrass, P., Mayer, C., Lengauer, B., Eckhart, L., Declerq, W., and Tschachler, E. (2002) Caspase-14 expression by epidermal keratinocytes is regulated by retinoids in a differentiation-associated manner. *J. Invest. Dermatol.* **119**, 1150–1155

66. Mildner, M., Ballaun, C., Stichenwirth, M., Bauer, R., Gmeiner, R., Buchberger, M., Mlitz, V., and Tschachler, E. (2006) Gene silencing in a human organotypic skin model. *Biochem. Biophys. Res. Commun*. **348**, 76–82

67. Xue, M. and Jackson, C. J. (2008) Autocrine Actions of Matrix Metalloproteinase (MMP)-2 Counter the Effects of MMP-9 to Promote Survival and Prevent Terminal Differentiation of Cultured Human Keratinocytes. *Journal of Investigative Dermatology* **128**, 2676–2685

68. Mercado, J., Pérez-Rigueiro, J., González-Nieto, D., Lozano-Picazo, P., López, P., Panetsos, F., Elices, M., Gañán-Calvo, A. M., Guinea, G. V., and Ramos-Gómez, M. (2020) Regenerated Silk Fibers Obtained by Straining Flow Spinning for Guiding Axonal Elongation in Primary Cortical Neurons. *ACS Biomater. Sci. Eng.*

69. Uebersax, L., Mattotti, M., Papaloïzos, M., Merkle, H. P., Gander, B., and Meinel, L. (2007) Silk fibroin matrices for the controlled release of nerve growth factor (NGF). *Biomaterials* **28**, 4449–4460

70. Mori, H., Oda, N., Abe, S., Ueno, T., Zhu, W., Pernstich, C., and Pezzotti, G. (2018) Raman spectroscopy insight into Norovirus encapsulation in Bombyx mori cypovirus cubic microcrystals. *Spectrochimica Acta Part A: Molecular and Biomolecular Spectroscopy* **203**, 19–30

71. Tan, M. and Jiang, X. (2014) Vaccine against norovirus. *Hum Vaccin Immunother* **10**, 1449–1456

72. Nardini, M., Perteghella, S., Mastracci, L., Grillo, F., Marrubini, G., Bari, E., Formica, M., Gentili, C., Cancedda, R., Torre, M. L., and Mastrogiacomo, M. (2020) Growth Factors Delivery System for Skin Regeneration: An Advanced Wound Dressing. *Pharmaceutics* **12**

Publication List

1. **Sustained Neurotrophin Release from Protein Nanoparticles Mediated by Matrix Metalloproteinases Induces the Alignment and Differentiation of Nerve Cells**

   Yuka Matsuzaki, Rina Maruta, Keiko Takaki, Eiji Kotani, Yasuko Kato, Ryoichi Yoshimura, Yasuhisa Endo, Ciara Whitty, Christian Pernstich, Raj Gandhi, Michael Jones and Hajime Mori. *Biomolecules.* 2019*,* 9, 510

2. **Effects of transgenic silk materials that incorporate FGF-7 protein microcrystals on the proliferation and differentiation of human keratinocytes**

   Rina Maruta, Keiko Takaki, Yuka Yamaji, Hideki Sezutsu, Hajime Mori, Eiji Kotani. *FASEB BioAdvances*. 2020, Volume 2*,* 734-744

3. **The Partial Purification and Biological Activity of FGF-2-encapsulating Cypovirus 1 Polyhedra Formed in the Silkworm Middle Silk Gland**

   Chiharu Honda, Rina Maruta, Keiko Takaki, Hajime Mori, and Eiji Kotani. *The Journal of Silk Science and Technology of Japan*. Vol. 28, 2020

4. Inhibitory effects of intact silkworm sericin on bacterial proliferation

Erica Matsumoto, Keiko Takaki, Rina Maruta, Hajime Mori, and Eiji Kotani. *The Journal of The Textile Institute*. 2020

Acknowledgements

The study presented in this Doctoral Dissertation was carried out under the guidance of Professor Eiji Kotani at Kyoto Institute of Technology.

I especially thank Prof. Eiji Kotani, Prof. Hajime Mori, and Dr. Keiko Takaki at Kyoto Institute of Technology for kindly teaching me for long time and valuable instruction. I thank Prof. Yoshihiro Inoue and Prof. Masanobu Itoh at Kyoto Institute of Technology for critical reading of the thesis. I thank Dr. Hideki Sezutsu at Institute of Agrobiological Sciences, National Agriculture and Food Research Organization for kindly providing silkworms. I am grateful to Dr. Ciara Whitty, Dr. Christian Pernstich, Dr. Raj Gandhi, and Dr. Michael Jones at Cell Guidance Systems for their helpful suggestions and collaboration. I thank Dr. Yasuko Kato, Dr. Ryoichi Yoshimura, and Prof. Yasuhisa Endo at Kyoto Institute of Technology for technical advice and helpful comments. I thank Ms. Yuka Matsuzaki, Ms. Yuka Yamaji, and Ms. Erica Matsumoto at Kyoto Institute of Technology for working together and their stimulating advices. I would like to thank all members at Insect Engineering laboratory, Kyoto Institute of Technology.